

A SPECTROSCOPIC ANALYSIS OF THE ENERGETIC TYPE IC ‘HYPERNOVA’ SN 1997EF

PAOLO A. MAZZALI^{1,2}, KOICHI IWAMOTO³, KEN’ICHI NOMOTO^{1,4}

To appear in the Astrophysical Journal

ABSTRACT

The properties of the bright and energetic Type Ic SN 1997ef are investigated using a Monte Carlo spectrum synthesis code. Analysis of the earliest spectra is used to determine the time of outburst. The changing features of the spectrum and the light curve are used to probe the ejecta and to determine their composition, verifying the results of explosion calculations. Since synthetic spectra computed using our best explosion model CO100 are only moderately good reproductions of the observations, the inverse approach is adopted, and a density structure is derived by demanding that it gives the best possible fit to the observed spectrum at every epoch analysed. It is found that the density structure of model CO100 is adequate at intermediate velocities (5000–25000 km s⁻¹), but that a slower density decline ($\rho \propto r^{-4}$) is required to obtain the extensive line blending at high velocities (25000–50000 km s⁻¹) which is the characterising feature of this and other energetic type Ic Supernovae. Also, the inner ‘hole’ in the density predicted by the model is found not to be compatible with the observed evolution of the spectrum, which reaches very low photospheric velocities at epochs of about 2 months. The ‘best fit’ density distribution results in somewhat different parameters for the SN, namely an ejecta mass of 9.6M_⊙ (v. 7.6M_⊙ in CO100) and an explosion kinetic energy of $1.75 \cdot 10^{52}$ erg (v. $8 \cdot 10^{51}$ erg in CO100). This revised value of the kinetic energy brings SN 1997ef closer to the value for the ‘prototypical’ type Ic ‘hypernova’ SN 1998bw. The abundance distribution of model CO100 is found to hold well. The modified density structure is used to compute a synthetic light curve, which is found to agree very well with the observed bolometric light curve around maximum. The amount of radioactive ⁵⁶Ni produced by the SN is confirmed at 0.13M_⊙. In the context of an axisymmetric explosion, a somewhat smaller kinetic energy than that of SN 1998bw may have resulted from the non alignment of the symmetry axis of the SN and the line of sight. This might also explain the lack of evidence for a Gamma Ray Burst correlated with SN 1997ef.

Subject headings: supernovae: general – supernovae: SN 1990N – line: identification – line: formation – line: profiles

1. INTRODUCTION

SN 1997ef in UGC4107 was recognised as a peculiar and interesting object as soon as its first spectra were taken by the Harvard-CfA team (Garnavich et al. 1997a,b,c). The spectra displayed very broad features, quite unlike those of any other SN known to date, so that it was not even clear whether what was observed was an absorption or an emission spectrum. Continued observation revealed a light curve typical of a SN deriving from a compact object (a SN Ia or a SN Ic), but much broader than the templates for both of these classes. Later spectra showed more resolved spectral lines, clarifying that the broad features were actually very extended absorption blends, and that the SN was therefore in the photospheric epoch. Lines of Ca II, O I and Fe II were strong, and the Si II 6347, 6371Å line appeared to be comparatively weak, so the SN was classified as type Ic, as also supported by the overall similarity with the spectra of other SNe Ic such as SN 1994I (Filippenko 1997; Millard et al. 1999).

Typical models for a low mass, low kinetic energy SN Ic (Nomoto et al. 1994; Iwamoto et al. 1994) gave good fits to the light curve, but the synthetic spectra computed using such models, while yielding the correct types of spectral

lines, completely failed to reproduce the observed large line width, which we estimated as at least 20000km s⁻¹ for some of the strongest lines (Iwamoto et al. 2000, hereafter Paper I).

Soon after SN 1997ef, however, the extraordinarily bright and powerful type Ic SN 1998bw was discovered as the optical counterpart of GRB980425 (Galama et al. 1998). A great deal of study, both observational and theoretical, was and still is being devoted to this SN, which was soon realised to be a massive type Ic event of exceptionally large kinetic energy ($KE \sim 3 \cdot 10^{52}$ ergs, Iwamoto et al. 1998; Woosley, Eastman & Schmidt 1999; Branch 2000), where the link with the GRB may lie in a rather asymmetric explosion (MacFadyen & Woosley 1999, Höflich et al. 1999, Khokhlov et al. 1999, Maeda et al. 2000). It was only natural then also to analyse SN 1997ef as a powerful ‘hypernova’. Paper I presents a detailed study of the light curve and the spectrum using two models, one for a ‘normal’ SN Ic (model CO60: M_{ej}= 4.4M_⊙, KE = 10⁵¹ erg) and another for a ‘hypernova’ (model CO100: M_{ej}= 7.6M_⊙, KE = 8 · 10⁵¹ erg). Both models have a ⁵⁶Ni mass of 0.15M_⊙. In Paper I we showed that both models reproduce the light curve reasonably well, but only the more

¹Research Centre for the Early Universe, School of Science, University of Tokyo, Bunkyo-ku, Tokyo 113-0033, Japan

²Osservatorio Astronomico, Via Tiepolo, 11, I-34131 Trieste, Italy

³Department of Physics, Nihon University, Chiyoda-ku, Tokyo 101-8308, Japan

⁴Department of Astronomy, School of Science, University of Tokyo, Bunkyo-ku, Tokyo 113-0033, Japan

massive and energetic model CO100 can also produce reasonable synthetic spectra, and therefore they opted for the ‘hypernova’ model and suggested that SN 1997ef may be a somewhat less extreme case than SN 1998bw. A possible connection with a GRB has been searched for in archives for SN 1997ef. The result was that GRB971115 could be compatible with SN 1997ef in position and time of occurrence (Wang & Wheeler 1998), but the statistical significance of the correlation is much weaker than for SN 1998bw and GRB980425.

In this paper, we concentrate on the spectroscopy of SN 1997ef. This is interesting in many respects. First, it is important that we not only fit the spectra and their evolution using one explosion model, but that we also understand which lines are present in the spectrum. Since we have available a sufficiently large number of observed spectra, we can follow the spectral evolution and thus probe different depths in the ejecta and verify the composition as a function of velocity, and also describe how the spectrum changes as a function of luminosity as the SN moves along the light curve. We use for this purpose the Monte Carlo (MC) code originally described in Mazzali & Lucy (1993) and further improved and discussed by Lucy (1999) and Mazzali (2000). The code includes the effect of photon branching, which must be very important in a situation where the high expansion velocities lead to extensive line blanketing. Also, since the code uses the bolometric luminosity as input, we can compare the required L values with those of a light curve calculation relaxing the assumption $BC = 0.0$ made in Paper I and thus improve the comparison between model L_{Bol} from light curve calculations and observed V mags.

Furthermore, we use spectrum synthesis to date the earliest spectra, and thus to determine with some accuracy the time of explosion, which is important for both the GRB connection and the light curve calculation.

Finally, having noticed that even synthetic spectra obtained from CO100 do not give wonderfully good fits to the observed spectra, we adopt the ‘inverse’ approach and try to determine the density and abundance distribution with velocity by looking for a best fit to the spectra. This method was pioneered by Branch (2000), who suggested for SN 1997ef a much flatter density dependence ($\rho \propto r^{-2}$) than what is predicted by model CO100 (where the density index is $n = -7$). Consequently, for SN 1997ef Branch (2000) obtains a much larger ejecta mass ($6M_{\odot}$ above $v = 7000 \text{ km s}^{-1}$) and kinetic energy ($3 \cdot 10^{52} \text{ erg}$ above the same velocity).

Since we study several spectra we can control ρ as a function of $v (= r/t)$, and hence build our own $\rho(r)$. We do confirm that the spectra require a flatter density dependence, but we show that this is only necessary at high velocity ($v > 25000 \text{ km s}^{-1}$). Examining spectra at advanced epochs, we also show that the predicted density ‘hole’ at low velocities is not compatible with observations. We therefore derive new values for both M_{ej} and KE .

We take this process one step further by computing a synthetic light curve from our derived $\rho(r)$, and show that this gives a very good fit to the observed light curve of SN 1997ef.

In the rest of this paper we first describe how we proceeded to date the spectra, then discuss the analysis of 6 spectra, reviewing the results and their implications. Then

we review the properties of the model for SN 1997ef as we derived it, and discuss how it differs from model CO100, which was computed to fit the light curve, not the spectra. We also show the synthetic light curve obtained from our ad hoc model for $\rho(r)$. Finally, we review and discuss our findings, including possible reasons why SN 1997ef was a hypernova but no GRB was apparently linked to it.

2. DATING THE SPECTRA

We have selected for modelling 6 spectra of SN 1997ef obtained by the Harvard-CfA group (Garnavich et al. in prep.; see Paper I, Figs. 8 and 9). We have chosen well exposed, high S/N spectra, with a large wavelength coverage, and tried to sample the light curve as uniformly as possible. The first three spectra are from epochs around maximum (which was not observed either spectroscopically or photometrically but was probably reached around Dec 10, 1997 at $V \sim 16.5$). The dates of the spectra are Nov 29, which is very soon after discovery, Dec 5 and Dec 17. All the spectra show very broad lines. They are all early enough that they are sensitive to changes in the kinetic energy and to the assumed epoch of outburst. The next two spectra have dates Dec 24 and Jan 1, which is around the time when the SN enters the tail of the light curve. The lines in these spectra becoming progressively narrower, indicating that the high velocity part of the ejecta is becoming optically thin. The final spectrum has date Jan 26, 1998, which is well on the light curve tail. Line velocities are quite small, suggesting that the spectrum is formed deep in the ejecta. One of the challenges for a good light curve calculation is to follow the evolution of the photospheric velocity with time. Even model CO100 was not perfect in this respect (cf. Paper I, Figure 7).

Since the epoch of maximum was not observed, light curve models are not very tightly constrained. Since the rise time to maximum depends on the structure of the model and the abundance distribution, the range of allowed parameters could be effectively constrained if at least the time of explosion could be determined, albeit with some uncertainty. This could be attempted using spectrum synthesis and the measured photospheric velocity as determined in Paper I from the velocity of the Si II line. It could be expected that this line is formed somewhat above the photosphere at very early epochs, like in SNe Ia (e.g. SN 1994D, Patat et al. 1996).

Since our synthetic spectra are computed using the luminosity L , the epoch t and the photospheric velocity v_{ph} as input, an appropriate value of t must be found that gives a photospheric radius $R_{\text{ph}} = v_{\text{ph}}t$ which, when combined with L , produces temperatures in agreement with the observed spectrum. In particular, although the continuum is not well determined in the very complex spectra of SN 1997ef, spectral lines serve a double role: they depend on the temperature (and hence on R_{ph} and L) through their ratios, and on v_{ph} through their displacement. Not many lines are visible in the earliest spectra, but at least Si II 6346, 6371Å and the broad complex which can most likely be identified as O I 7774Å, O I 8447Å and the Ca II IR triplet could be used to guide the calculation of the synthetic spectra.

Models for Nov 29 show that acceptable fits are found for $t = 7-9$ days and $v_{\text{ph}} = 18000-15500 \text{ km s}^{-1}$. Greater epochs require smaller velocities, so that R_{ph} always has

a value of about $1.1 \cdot 10^{11}$ cm. This radius, combined with the value of L , which depends almost entirely on the assumed distance, gives a temperature appropriate to get a good overall fit to the spectrum. If we assume e.g. $t = 11$ days, then we find a good overall fit to the spectrum for $v_{\text{ph}} = 13500 \text{ km s}^{-1}$, which is too small and is reflected on the line shift. The opposite happens if $t \leq 7$ days. In order to strengthen our result, we applied the same technique to the Dec 5 spectrum, and we found acceptable fits for $t = 14 - 15$ days and $v_{\text{ph}} = 10000 - 9500 \text{ km s}^{-1}$. Therefore, the two epochs give consistent results, and we can estimate the time of outburst to have been Nov 20–22. Since the fits obtained for $t = 9$ days on Nov 29 and $t = 15$ days on Dec 5 were particularly good, we selected Nov 20 as our reference epoch, also for the comparison with the light curve and the photospheric velocities. We will show the fits in the next sections, when discussing the various epochs. In Figure 1 we show as an example the Nov 29 spectrum and two synthetic spectra computed as above for $t = 9$ days (dashed line) and $t = 11$ days (dotted line), respectively, using model CO100. The difference in velocity is clearly visible.

These results depend on the selection made for two other quantities, distance and overall ejecta mass, as discussed by Mazzali & Schmidt (2000) in the context of Type Ia SNe. For all models, we adopted a distance modulus of 33.63, i.e. a distance of 53.1 Mpc, as estimated from a recession velocity of 3450 km s^{-1} (P. Garnavich, 2000, private communication) and $H_0 = 65 \text{ km s}^{-1} \text{ Mpc}^{-1}$. We assume no extinction ($E(B - V) = 0.0$), which is justified by the absence of a narrow interstellar Na I D line from the spectrum of SN 1997ef at all phases. As for the ejected mass, we already showed in Paper I that this must be large in order to fit both the light curve and the spectra. Therefore in this paper we use the solution found in Paper I, model CO100, as a reference.

3. THE 29 NOVEMBER 1997 SPECTRUM

This is to our knowledge the earliest spectrum available of SN 1997ef. Although it is somewhat noisy and it does not extend very far to the red, it nevertheless includes most of the main features, which made SN 1997ef such a peculiar and interesting object. The spectrum (Figure 2) has essentially no continuum, and it is characterised by four broad minima, at roughly 3900, 4700, 6000 and 7500 Å. The minima are separated by three rather sharp peaks, at 4300, 5200 and 6300 Å, respectively. The minima are so broad and the peaks so strong that the spectrum could be confused for an emission spectrum. Both Branch (2000) and Paper I showed that the real nature of the spectrum is a superposition of absorption lines. We already pointed out that the ‘emission peaks’ are the result of photon travel in a medium of large line opacity. Photons redshift their way through the envelope until they find a portion of the spectrum where line opacity is low because of the intrinsic distribution in wavelength of the atomic transitions. We call such a region a ‘line-free window’. A large number of photons escape through these regions - all the photons coming from the optically thick region immediately to the blue, and this leads to a large flux and to the observed ‘peaks’. While the width of the peak depends solely on the width of the line-free window, its strength depends both on the flux at the lower boundary (the photosphere) and

on the width of the blanketing region which feeds photons to it: the broader the blanketing region, the more photons must reach the window to escape, resulting in a higher peak flux. This can be easily seen by inspection of the spectrum.

In Paper I we showed that a synthetic spectrum based on model CO100 gives a reasonably good reproduction of the observations, and allows us to identify the four absorptions as follows: 3900 Å: Ca II H&K + Ni II, Co II and Si II lines; 4700 Å: mostly Fe II lines; 6000 Å: Si II 6347, 6371 Å plus weaker Si II lines and Na I D further to the blue; 7500 Å: O I 7774 Å. In spectra computed with model CO100 the O I 7774 Å and the Ca II IR triplet are well separated, but unfortunately the observed spectrum does not extend far enough to the red to show the Ca II region. With reference to that synthetic spectrum, which is shown again here as the dashed line in Figure 2, we notice that none of the absorptions extend quite far enough to the blue. For the two bluer troughs, which are blends of very many lines, this may possibly be due to the lack of lines resulting from neglecting some element or not using a sufficiently complete line list, but this seems unlikely for the two redder troughs, where a few very strong lines dominate.

The synthetic spectrum has $t = 9$ days, $\log L = 42.13$ (erg s^{-1}), $v_{\text{ph}} = 15500 \text{ km s}^{-1}$. The observed V magnitude (16.7) and the synthetic one (16.75) agree quite well, but the spectrum has a large Bolometric Correction (0.28), which indicates that the assumption $BC = 0.0$ made in Paper I when fitting the light curve is at least weak. The observed Si II line velocity is 19000 km s^{-1} , and the core of the Si II absorption is well reproduced even using model CO100. Therefore, in order to improve the synthetic spectrum, we modified the density only above 20000 km s^{-1} . While the original CO100 model has $\rho \propto r^{-8}$ in the outer part, we made the outer density radial dependence flatter. As a consequence, high velocity absorption becomes stronger. Of course, this happens first in the strongest lines, the Ca II H&K doublet and IR triplet first and foremost. The strength of these lines increases dramatically, because they come from low excitation levels which are still highly populated even at the very low densities and temperatures of the outer envelope ($T_e \sim 4000 \text{ K}$), and so these lines increase greatly in width. Next come the Si II and O I lines. For these lines, the drop in the level population with radius is much steeper, since they come from levels on average about 10 eV above the ground state, and so they do become broader, but not so noticeably, and their cores do not shift much towards the blue. All other lines, strong and weak are similarly affected, to a higher or lesser degree depending on the ionisation and excitation of the levels.

Since we wanted to introduce as little change from model CO100 as possible, we choose the steepest density profile which gave a good fit to the spectrum. This was obtained with a density power law index $n = -4$ at $v > 25000 \text{ km s}^{-1}$. When this change is introduced the Ca II H&K doublet, the Si II line and the O I 7774 Å line broaden to the point that the observed absorption troughs are very well reproduced. Further to the red, in the unobserved part of the spectrum, the Ca II IR triplet is predicted to broaden and blend with O I 7774 Å. The contribution of O I 8446 Å, which is also a strong line, is

nevertheless small compared to that of Ca II. The blending of O I 7774Å and the Ca II IR triplet is an important discriminant for the density structure at high velocities. Fortunately, the Dec. 5 spectrum covers that region. The blue sides of the peaks at 4300 and 5000Å are also fitted much better, as the increased density causes the emission to set in at higher velocities.

The only region where no improvement is seen is near 4500Å. The Fe II and Co II lines causing the absorption near 4750Å are not sufficiently strong to extend to the blue, and there are not enough strong lines that absorb near 4400–4500Å. It is possible that we are either missing lines or ignoring some relevant element. Interestingly, Branch (2000), who used a code that is very efficient for identifying lines, seemed to have the same problem.

The modification to the outer density profile has only a small influence on the total mass, since it adds only about $0.25M_{\odot}$ in the outer ejecta, but it does lead to a significant increase in the overall kinetic energy, since all the mass is added to the high velocity shells, where it represents a dramatic increase, of 1–2 orders of magnitude. The kinetic energy above 20000 km s^{-1} increases from 10^{51} to about 10^{52} erg, and the total kinetic energy increases from $8 \cdot 10^{51}$ to $1.75 \cdot 10^{52}$ erg. This is quite a large change, but it is still smaller than the value adopted for SN 1998bw. Also, both the outer slope and the revised *KE* are, respectively, steeper and smaller than the values suggested by Branch (2000). We will discuss the implications of these revised values later. An increase in *KE* only makes SN 1997ef more like a hypernova.

The best fitting ad hoc model has the same input parameters as the spectrum computed using CO100. The increased outer density makes the temperature only slightly higher. The synthetic spectrum has $B = 17.45$, $V = 16.74$ and $BC = 0.29$, so that $M_{Bol} = -16.70$. Therefore comparing M_{Bol} with V is misleading, since V rises more rapidly than M_{Bol} .

Finally, a word of comment about the presence of He in the spectrum. In SN 1998bw, He I 10830Å was almost certainly observed in absorption at early epochs (Patat et al. 2000). Its presence could be understood if the He shell was not completely lost before the explosion. Unfortunately, IR spectra are not available for SN 1997ef, so the best place to look for He is He I 5868Å. This line is very close to Na I D, which is rather strong and contributes to the broad 6000Å trough with an absorption near 5450Å. A small He mass does not produce a strong line unless very large departure coefficients are assumed, and in any case a strong He I line is not necessary to fit the spectrum. Therefore, although we cannot be final, we do not think He I 5868Å is present in the Nov 29 spectrum.

4. THE 5 DECEMBER 1997 SPECTRUM

The second spectrum in our analysis has a good S/N and a very good wavelength coverage, extending from 3100 to 8700Å. It is actually quite similar to the 29 Nov. one, but more detail is visible (Figure 3), e.g. the structure of the complex 6000Å absorption and, very importantly, the Ca II IR triplet is visible, and clearly blended with O I 7774Å, which is a strong argument in favour of a ‘flat’ outer density distribution, as discussed above. That the feature measured at 7500Å is a blend is clear, given the

presence of two distinct absorptions, whose wavelengths match those of the two component multiplets, as shown also by the spectrum computed with model CO100.

The synthetic spectrum based on model CO100 was shown in Paper I and again here as the dashed line in Figure 3. It has parameters $t = 15$ days, $\log L = 42.15$ (erg s^{-1}), $v_{ph} = 9500 \text{ km s}^{-1}$. Both L and R_{ph} have values similar to those on Nov. 29, therefore the temperatures are similar and so are the two spectra, although the photosphere is quite a bit deeper on Dec. 5. This is shown also by the Si II line velocity, which is reduced to 13000 km s^{-1} . The observed V mag on Dec 5 was 16.5, and the CO100 spectrum reproduces it well ($V = 16.63$). The problem with that model is essentially the same as that discussed for the Nov 29 model: all troughs do not extend far enough to the blue. Furthermore, O I 7774Å and the Ca II IR triplet do not blend anywhere near as much as they should when the original model is used. In that spectrum the Ca II IR triplet extends only to about 7850Å, i.e. a Ca II velocity of $\sim 25000 \text{ km s}^{-1}$. If the Ca II IR triplet is to blend with the O I line, it must reach at least 7650Å in the blue wing, i.e. $v \sim 31000 \text{ km s}^{-1}$. This is consistent with the modified density structure adopted for the Nov 29 spectrum. Since v_{ph} is much lower than the values at which the density has been modified ($v > 20000 \text{ km s}^{-1}$), we can use the same density structure as for Nov 29.

The spectrum we computed for the modified structure and the same input parameters as above is shown in Figure 3. The improvements are apparent, and they concern mostly the Ca II IR triplet + O I 7774Å feature in the red and the blue region near 4000Å, which is improved by the strengthening and broadening of Ca II H&K. Improvements in the trough at 4700Å are again only marginal, as are those to the Si II line region. Surprisingly perhaps, the Si II line does not become broader, but this can be understood since the high velocity regions where the density has been enhanced are far above the photosphere and are of too low density now to cause much Si II absorption. The situation is made more complicated by the apparent development of an absorption shoulder near 5900Å. We cannot offer a clear identification for this shoulder, except for several lines of O I at 6157Å, but these are not very strong. The shoulder was not present on Nov 29, nor is it on Dec 17. Another, stronger shoulder is visible near 5750Å. This is where Si II 5958, 5979Å falls, and the synthetic spectra show that this doublet, combined with Na I D further to the red, is strong enough to produce a shoulder stronger than the observed one without resorting to He I. Therefore we can confirm the non-detection of He I 5876Å. Note that the Si abundance in this model was lower than on Nov 29. This was necessary to fit the core of the Si II 6347, 6371Å line. Even the modified density does not give a perfect synthetic spectrum, but the excellent behaviour in the red confirms that we are adopting the correct measures when using an extended outer envelope.

If a density law flatter than $n = -4$ is adopted in an attempt to improve the Si II line two problems emerge: 1) O I 7774Å extends too far to the blue and 2) the increasing strength of Ca II H&K causes too much blocking of the UV spectrum and, consequently, a synthetic peak at 4500Å much stronger than what is observed. These problems would be even worse in the Nov 29 spectrum, and so

we chose to retain the $n = -4$ solution as a compromise and suggest that some alternative line may be the reason for at least the shoulder at 5900\AA .

Our best-fitting spectrum has $B = 17.53$, $V = 16.58$ and again a large $BC = 0.40$, so that $M_{Bol} = -16.75$. The increased BC is apparent if one looks at the ratio of the two main peaks, at 4300 and 5200\AA . Therefore, M_{Bol} is significantly smaller than V at this epoch, which is near maximum in the V light curve but appears to be still very much on the rising branch of the bolometric curve.

5. THE 17 DECEMBER 1997 SPECTRUM

This third spectrum has again a limited wavelength coverage, but it is the first one available after Dec 5, and it is therefore useful to study the evolution of the SN immediately following V maximum. The spectrum, which is displayed in Figure 4 has $V = 16.6$. The overall aspect of the spectrum is similar to the previous two epochs, which indicates that the temperature conditions have probably not changed greatly.

However, closer inspection, and in particular a wavelength comparison of this and the two earlier spectra, reveals that all the main absorption and emission peaks have shifted to the red by $100\text{-}200\text{\AA}$, depending on the wavelength. A similar, but smaller shift also occurred between Nov 29 and Dec 5. The immediate interpretation is that we are observing the effect of the inward motion of the photosphere through the ejecta as they expand and thin out. Note that this recession takes place essentially in the lagrangian mass/velocity frame, and not in the observer's (radius) frame, much like in the Plateau phase of some SNe II. The Si II velocity measured from this spectrum is in fact only 8000km s^{-1} . The change in line absorption velocity is larger between Dec 5 and Dec 17 than it was between Nov 29 and Dec 5 because the time interval between the spectra is larger. All absorptions move by about the same amount, and the emissions move as well. This is obvious given our explanation for what the emissions really are: if the blanketed regions move, the opacity windows must move along with them, just like in P-Cygni profiles caused by a single line, a situation of which the case of SN 1997ef represents after all just an extreme extension. Looking in more detail, the shoulder which affected the Si II line near 5900\AA on Dec 5 seems to have disappeared on Dec 17, leaving serious questions about its identity. The absorption near 5000\AA now shows more structure, with minima at 4800 and 4950\AA and two shoulders at 5100 and 5300\AA , which resembles quite closely the typical profile observed in SNe Ia near maximum and soon thereafter. In SNe Ia the entire feature is attributed mostly to Fe II lines, and this was confirmed in SN 1997ef on both Nov 29 and Dec 5.

The synthetic spectrum computed with CO100 is shown as the dashed line in Figure 4. The structure in the Fe II absorption is reproduced reasonably well, and the width problem now does not affect either the feature at 4300\AA or that near 7500\AA . This is probably because the outer high velocity regions are so far above the photosphere now that they do not really cause any significant absorption, and so the original model CO100 gives an acceptable description of the density structure in the intermediate velocity regions. Unfortunately this spectrum does not cover the Ca II IR triplet, which is predicted not to blend with O I

7774\AA in the CO100 model. The synthetic spectrum was computed with the following parameters: $t = 27$ days, $\log L = 42.20$ (erg s^{-1}), $v_{ph} = 7500\text{km s}^{-1}$. The temperatures are lower than on Dec 5 but comparable to those on Nov 29, and R_{ph} is actually larger than on both previous epochs, although the mass above the photosphere is now as large as $5M_{\odot}$. Compared to the Dec 5 model, the abundance of O is reduced and that of S increased, which is the behaviour expected as deeper and deeper regions of the ejecta are probed. The reduced velocity is the reason for the de-blending of many features. There are two major shortcomings in the model: 1) the position of the peak at 5500\AA is not correctly reproduced. This is clearly the consequence of the absorption at 5400\AA not being correctly reproduced, so that the 'optical depth window' starts too far to the blue. This feature is not well reproduced in the spectra of SNe Ia either, so it is quite likely that some Fe-group lines are missing or their strength is not correct. 2) The Si II line is too narrow, or rather the very triangular shape of the blue side of the absorption cannot be reproduced. Only another Si II line is active in that region (Si II 5979\AA , observed near 5800\AA), but it is too weak. In any case it would be difficult to explain the observed profile with just one line, so we really have no explanation for what might affect the spectrum.

We have also modelled the spectrum using our modified density distribution (Figure 4, continuous line). As we could expect, since the near-photospheric region is not affected by the modification, at this epoch the two synthetic spectra are essentially identical. The spectrum computed with the modified outer density profile has $B = 17.73$ and $V = 16.66$. The bolometric correction is still large, $BC = 0.20$, and $M_{Bol} = -16.87$. It is very interesting that the model luminosity, as obtained from fitting the spectrum, is actually larger on Dec 17 than on Dec 5. The bolometric light curve appears then quite different from both the V and the B curves. The large bolometric correction is now caused mostly by the red part of the spectrum, with the synthetic R band still rising so that the bolometric light curve rises slowly to a rather delayed maximum. Near-IR photometry would have been useful to confirm this prediction.

6. THE 24 DECEMBER 1997 SPECTRUM

The 24 Dec spectrum is the first of a set of three spectra modelled in this paper which extend the time coverage beyond the near-maximum epochs considered also in Paper I. The 24 Dec spectrum is shown in Figure 5. It does not extend far to the red, but in the blue it has a good S/N down to 3700\AA , thus covering the Ca II H&K region. The epoch of the spectrum is 35 days after explosion, for which we chose Nov 20. The spectrum has $v = 16.8$, a drop of 0.2 mag in only one week from Dec 17, and lies therefore well in the declining part of the V light curve. The Si II line is now quite narrow, and its core has a velocity of 5400km s^{-1} . This and all other absorptions continue to move to the red. Following the trend already noticeable on Dec 17, many small features which earlier blended into the broad troughs are beginning to be resolved, marking the progressive inward motion of the photosphere. The broad absorption near 6000\AA is the region that changed the most with respect to Dec 17. In particular, a separate

absorption is now visible at 5700Å.

We modelled the spectrum using model CO100 with the outer modification introduced as discussed above. As usual, L and v_{ph} were selected so as to get as good a fit as possible to the observations. The input parameters for the best model, which is shown as the continuous line in Figure 5, were $t = 34$ days, $\log L = 42.13$ (erg s $^{-1}$) and $v_{\text{ph}} = 4900\text{km s}^{-1}$. Note that L has the same value as on Nov 29, indicating that the bolometric light curve is now declining. The photospheric velocity is now very low, as is also indicated by the Si II line velocity, and is actually slightly below the inner edge of the density distribution of model CO100 (cf. Paper I, Figure 3). Therefore, in order to produce a reasonable spectrum we had to introduce a second change to the CO100 density structure, extending it down to v_{ph} . We used $\rho \propto r^{-1}$ for this inner extension. This is only a first approximation, but it is obvious that if there is a photosphere there must be opacity right down to it, and this is not compatible with the ‘density hole’ predicted by model CO100 below 5300km s $^{-1}$. Since the photosphere is so deep, the inclusion of the flat outer density profile derived from the earlier spectra has no effect on the synthetic spectrum. Even when the flat outer density is included, O I 7774Å and the Ca II IR triplet are predicted to be separated in wavelength. This region is not covered on Dec 24, but our prediction will be confirmed in the Jan 1 spectrum (see next section). The small inner extension to the density does not affect the total mass much, so that at this epoch the total mass above the photosphere is $8.4M_{\odot}$.

A major change in this model is in the abundances. As shown in Figure 7 of Paper I, the Oxygen-dominated envelope extends down to 6500km s $^{-1}$. On Dec 24 the photosphere is well below this point, and Si, S and the Fe-group have larger abundances. We fitted the abundances to obtain a best fit, and found that S is the element whose abundance must increase most, at the expense of O. The behaviour of the abundances as determined from spectrum synthesis is reviewed in the discussion. Most line identifications are the same as on earlier epochs. The absorption at 5700Å is due to Na I D. Overall, the synthetic spectrum is a good match to the observed one. The major shortcoming is that the emission peak near 6500Å is not reproduced. Net emission may be present there, although the wavelength does not match that of the expected line of [O I] 6300Å. There is a wavelength coincidence with H α , but this is not expected to be a strong feature in a SN Ic ejecta.

The synthetic spectrum has $B = 17.83$ and $V = 16.71$. The bolometric correction is still large, $BC = 0.32$, so that $M_{\text{Bol}} = -16.70$. Therefore, it appears that bolometric maximum was reached near Dec 24, much later than V or B maximum. A lot of the flux is still released in the near-IR, in particular in the Ca II IR triplet peak.

7. THE 1 JANUARY 1998 SPECTRUM

The next spectrum in our series is rather close in epoch to the previous one but, with an epoch of 42 days, it captures a moment when the light curve begins to settle on the tail. Although the S/N is only moderately high, the ample wavelength coverage (3400 to 8900Å) makes it an interesting spectrum to model. The spectrum is shown in

Figure 6. Comparing it to the Dec 24 spectrum, several signs of development can easily be noticed:

1. The ratio of the three peaks in the blue, at 4000, 4500 and 5500Å is much steeper, indicating a shift of the flux towards the red which clearly must be the consequence of a reduced temperature.
2. The absorption complex near 6000Å has now split into two components. One is centred near 5700Å and is due to Na I D, which is now sufficiently strong and isolated because of the reduction in strength of neighbouring lines coming from more highly excited levels that it gives rise to its own P-Cygni emission, near 5900Å. To the red of Na I D the Si II line is still strong, near 6250Å, and is accompanied by a weaker absorption near 6100Å, which was also present on Dec 24.
3. Two absorptions are developing at about 6800 and 7100Å.
4. The O I 7774Å line and the Ca II IR triplet are now well separated, as was already predicted by our synthetic spectrum on Dec 24. The O I line is rather narrow, while the Ca II absorption is broader. This is a consequence of the different run of excitation with radius (excitation falls more steeply for O than for Ca, and so does the line optical depth).
5. Emission in the Ca II IR triplet is now very strong, much stronger than the corresponding absorption: this indicates that net emission is beginning to be an important contribution to spectrum formation.
6. The line blueshift is further reduced: the Si II line now has a measured $v = 3600\text{km s}^{-1}$. This is now significantly smaller than than the inner boundary of the original CO100 density distribution. Since the essentially photospheric nature of the spectrum is proved by the progressive evolution of all features, a viable model must include a low velocity extension to the density profile.

Therefore, we modelled the spectrum using as a starting point the CO100 density distribution modified at high velocity as described earlier. This modification has no effect on the emerging spectrum at these later epochs: the maximum observable matter velocity, measured at the blue edge of the Ca II IR triplet is only 23000km s $^{-1}$. We extended the density distribution inwards to $v = 3000\text{km s}^{-1}$, and tried various density laws below 5000km s $^{-1}$. Our first conclusion is that the density must be increasing inwards: if we use a decreasing density a shell forms near 5000km s $^{-1}$ which affects the lines; if the density is constant below 5000km s $^{-1}$ the value near the photosphere is too low and the lines are too weak. On the other hand, if the density increases too steeply the synthetic lines tend to be too sharp. As a best approximate solution we adopted a power law with $\rho \propto r^{-1}$.

Our final model has parameters $t = 42$ days, $\log L = 42.0$ (erg s $^{-1}$), $v_{\text{ph}} = 3600\text{km s}^{-1}$, which is close to the observed Si II velocity. It is interesting that the simultaneous reduction in both L and v_{ph} means that the electron temperature T_e ranges between 4500 and 6500K, which is close to the values it had on previous epochs. This explains

why the nature of most line features is unchanged throughout the evolution of the SN. The synthetic spectrum is shown as the thin line in Figure 6. Overall, the quality of the fit is rather good, confirming the correctness of our assumption. Major shortcomings are: 1) the strength of the peak at 4500Å. This is probably due to having somewhat too much opacity in the UV. 2) The strength and position of the peak near 5500Å. This was a problem also on Dec 24 and we explained it as the consequence of missing line strength near 5400Å. 3) Flux is missing in the Ca II IR triplet emission. This is because net emission - following collisional excitation - is not included in our code. The difference between the observed and synthetic peak is to be ascribed to net emission, which is responsible for about half of the total line flux.

Other parts of the spectrum are very well reproduced, e.g. the O I and Ca II IR triplet absorption, the structure of the Si II line region, where the weak absorption at 6000Å is attributed to Fe II 6148Å and the emission near 6500Å is now correctly reproduced, confirming that the peak on 24 Dec was probably not [O I] 6300Å. The weak absorptions at 6800 and 7100Å correspond to lines of O I 7001Å and to several Fe II lines, respectively, but the synthetic lines are too weak. Fe II lines are becoming stronger as the abundance of Fe-group elements is higher, while that of O is further decreased.

The inward extension of the density affects the ejecta mass, adding about $1.5M_{\odot}$ between 3000 and 5000km s⁻¹, but it only has a small effect on the kinetic energy, adding only $2 \cdot 10^{50}$ erg in that velocity shell. The synthetic spectrum has $V = 17.16$, which compares well with the observed $V = 17.3$. Synthetic $B = 18.41$, showing that the spectrum is rather red. The R magnitude drops less than both B and V , and the bolometric correction is still large, $BC = 0.22$, so that $M_{Bol} = -16.35$, but this neglects the net emission in the Ca II IR triplet, so the actual value is probably smaller.

8. THE 26 JANUARY 1998 SPECTRUM

This is the last spectrum available, corresponding to an epoch well on the light curve tail, with $V \sim 18.0$. The spectrum, shown in Figure 7, shows a clear evolution from Jan 1. In particular, the flux peak has moved to the red quite noticeably, indicating a temperature drop. Looking at the spectrum in detail, one can notice that the features in the blue have changed little, and so has the region furthest to the red, although the Ca II IR triplet emission is now stronger. On the other hand, the region around 6000Å has changed quite significantly. The flux peak has moved from 5500 to 6000Å, the absorptions at 5700Å (Na I D) and at 6200Å are much stronger. The Si II line has essentially disappeared, all that is left being a weak feature near 6400Å, which is too red to be identified with the Si II doublet. In fact, a Si II velocity cannot be measured at this epoch. Still, many features have persisted from earlier epochs, and these have shifted further to the red, indicating the presence of significant amounts of material at very low velocity in the ejecta.

The overall nature of the spectrum is still photospheric, but the incidence of net emission is higher than on Jan 1, which will limit our ability to fit the spectrum using the MC code. We used the density distribution discussed

in the previous section, including both the outer $\rho \propto r^{-4}$ part above 25000km s⁻¹, which has no effect on the synthetic spectrum, and the inner $\rho \propto r^{-1}$ extension between 3000 and 5000km s⁻¹, but we had to extend the density distribution further inwards, so that we could obtain an appropriate temperature and spectrum. In keeping with the hydrodynamical prediction of a ‘density hole’ in the centre of the ejecta, we tried to use the largest possible value of the density power law index allowed by the quality of the synthetic spectrum. We selected a model based on the overall fit, but we could not reproduce the observations as well as on previous epochs. We could accommodate an innermost density law $\rho \propto r$ below 3000km s⁻¹, which is an attempt to include an inner ‘hole’ in density. This extension adds a further $0.5M_{\odot}$ to the ejecta mass, but only less than 10^{50} erg to the explosion kinetic energy. Our best fit spectrum, shown in Figure 7, has parameters $t = 67$ days, $\log L = 41.80$ (erg s⁻¹) and $v_{ph} = 1950$ km s⁻¹. The temperature is significantly lower than on Jan 1, with T_e ranging from 6000 to 4000K. Because of the rather flat density structure at low velocity, the temperature is almost constant ($T_e \sim 6000$ K) at $v \leq 6000$ km s⁻¹, which is where the spectrum is formed. This helps to keep the lines sufficiently broad. The abundances are similar to those of Jan 1, but Oxygen is further reduced and S is increased, reflecting the expected trend as smaller and smaller velocities are sampled.

Admittedly, the synthetic spectrum is not a very good fit, but almost all the observed features are at least reproduced. The two emission peaks at 4600 and 5500Å are much too strong in the model, which affects the synthetic V magnitude. The observed value is $V = 18.0$, and the synthetic spectrum has $V = 17.85$. The B flux is also somewhat overestimated at $B = 19.06$. Possible reasons for the excessive strength of the synthetic peaks at 4600 and 5400Å were already given in the previous section. In the V region, an absorption near 5600Å is also not reproduced. A similar feature was also observed on Jan 1, near 5650Å, but it was weaker then, while it was absent on Dec 24.

The absorption might be attributed to He I 5876Å at a velocity of about 13000km s⁻¹. He may be expected to be found in the ejecta as a leftover of the star’s He-shell. If He is distributed in a shell, He atoms may only be excited at a rather advanced epoch, when the γ -rays and positrons from the decay of ⁵⁶Co can penetrate the ejecta and reach the shell. However, the velocity implied by the position of the absorption is low for a hypothetical He shell, and the apparent shift of the feature between Jan 1 and Jan 26 does not support this scenario either. Alternatively, He can be produced with ⁵⁶Ni in the deepest layer as the result of alpha-rich freezeout (see Paper I, Figures 5 and 6). In this case He would be found together with Co/Fe, so the He velocity could take any value depending on the ⁵⁶Ni mixing. However, in this case non-thermal excitation of He would take place immediately, and we should see the He I line as soon as the photosphere reaches the layer where He is present. If He is located at about 14000km s⁻¹, we should have seen the He I line as early as Dec 5. The above problems notwithstanding, as long as no other candidate identification is available He must be regarded as at least a possibility. Observations of He I 10830Å would certainly help settle this issue. In any case, given the moderate

strength of the line, the He mass involved may not have to be large.

The model predicts a moderately strong absorption at 6300Å, attributing it to a blend of the Si II doublet and, mostly, of Fe II 6417, 6456Å. This feature is present also in the observed spectrum, but it is much weaker. The reason for the discrepancy is clearly the emission at 6300Å, which must signal the onset of the corresponding [O I] line. Another net emission, which is not reproduced by the model, is visible near 7300Å. This is clearly Ca II] 7292, 7324Å. Together with the Ca II IR triplet, these are the only three net emissions in the optical spectrum. This is a typical situation for SNe Ic at these epochs (cf. SN 1987M at 60 days after maximum, Swartz et al. 1993).

Comparing the spectra of SN 1997ef and SN 1987M, apart from the obviously broader lines in SN 1997ef, it is possible to note that in SN 1987M the Fe II lines are weaker and that the candidate He I line is not seen. SN 1987M is thought to have produced roughly as much ^{56}Ni as SN 1997ef ($0.15M_{\odot}$; Nomoto, Filippenko, & Shigeyama 1990, Paper I), but this could be an overestimation. Classical, low energy SNe Ic are not expected to eject any He, but this might not be the case for SN 1997ef, and it certainly is not for the other hypernova, SN 1998bw, where He I 10830Å is observed (Patat et al. 2000). On the other hand, at a comparable epoch the [O I] 6300Å emission is much stronger in SN 1998bw than in SN 1997ef, supporting the idea that SN 1998bw came from a more massive progenitor. Further detailed study of the He (and O) content of hypernovae would certainly be worthwhile.

The synthetic spectrum has a small BC (0.01), and $M_{Bol} = -15.87$. The actual value of BC may be even smaller, and possibly negative, since the model V flux is certainly overestimated by about 0.15 mag, and the net emission in the Ca II IR triplet is not included in our estimate. Therefore, the value of M_{Bol} has an uncertainty of at least 0.2 mag.

9. THE EXPLOSION PROPERTIES OF SN 1997EF

As we have discussed above at great length, modelling the time evolution of the spectrum of SN 1997ef has revealed two main inconsistencies with the explosion model CO100, which we used in Paper I to reproduce both the light curve and the near-maximum spectra. The basic parameters of the observed and synthetic spectra are recapped in Table 1.

Firstly, the high line velocities observed near maximum in several strong lines, notably the Ca II IR triplet and the Si II doublet, could not be reproduced with the rather steep density profile of CO100, but require a flatter outer density law, $\rho \propto r^{-4}$, at $v > 25000\text{km s}^{-1}$.

Secondly, the fact that the January spectra are still predominantly photospheric in nature, showing low line velocities ($v < 5000\text{km s}^{-1}$) is not compatible with the presence in CO100 of an inner ‘density hole’. This ‘hole’ was the result of depositing the kinetic energy at a radius in the progenitor which results in the ejection of exactly the amount of ^{56}Ni necessary to reproduce the SN tail luminosity. Matter below that radius, known as the ‘mass cut’, is assumed to fall back onto the compact remnant. Clearly, material must exist at low velocities, and we found that an inner extension below 5000km s^{-1} with a $\rho \propto r^{-1}$ den-

sity law down to 3000km s^{-1} and a $\rho \propto r$ law below that, to reproduce the inner ‘density hole’, is the best overall solution, although we still cannot get perfect fits of those very late epochs, even ignoring the net emission which is clearly present in some lines.

In Figure 8 we show the density profile of the original CO100 model and our modified one. The outer density extension adds significantly to the kinetic energy ($\sim 10^{52}\text{erg}$), but only marginally to the ejecta mass ($0.25M_{\odot}$), while the inner extension adds about $1.65M_{\odot}$ to M_{ej} but has a negligible effect ($\sim 2 \cdot 10^{50}\text{erg}$) on the explosion kinetic energy. Our modified model has a total $M_{ej} = 9.5M_{\odot}$ and $KE = 1.9 \cdot 10^{52}\text{erg}$, compared to $M_{ej} = 7.6M_{\odot}$ and $KE = 8 \cdot 10^{51}\text{erg}$ for CO100. These new values reinforce the classification of SN 1997ef as a hypernova, which is based on the KE being larger than 10^{52}erg .

Since we have a $\rho \propto r^{-4}$ density law on the outside, and an essentially flat law deep inside, and since our density distribution was derived starting from that of CO100, whose relic is the steep density gradient in the intermediate part, one might argue that a $\rho \propto r^{-4}$ density law might work well throughout the ejecta. We have tested such a possibility, but although it works reasonably well for the outer part, at $v \sim 20000\text{km s}^{-1}$, it gives rise to very sharp-lined spectra at the later epochs, when the photosphere is in the flat part of the ejecta, at $v < 10000\text{km s}^{-1}$. Also, joining directly the inner flat part and the outer $\rho \propto r^{-4}$ part beyond 10000km s^{-1} would give a SN with extremely large M_{ej} and KE , and the synthetic spectra for the epochs when the photosphere is near 10000km s^{-1} would have very deep lines.

We have to ask ourselves the question what could give rise to the observed deviation from the hydrodynamical model. The flat outer part may be due to mass loss at high rate during the presupernova stages, or to a transition between the Oxygen shell and an outer Helium shell, some evidence for which may be present as a weak He I 5876Å line in the two January spectra, although at a velocity ($\sim 13000\text{km s}^{-1}$) which is smaller than what would be expected. Branch (2000) offered a similar solution, and his ad hoc density law was even flatter $\rho \propto r^{-2}$ than ours. As a result he offers an estimate of the kinetic energy above 7000km s^{-1} as $3 \cdot 10^{52}\text{erg}$. Our value above the same velocity is somewhat smaller but comparable, $1.8 \cdot 10^{52}\text{erg}$. Also, he suggests that the ejecta mass above 7000km s^{-1} is $\sim 6M_{\odot}$, and our value is again smaller but comparable, $\sim 4M_{\odot}$.

The location of the inner density cutoff, on the other hand, was determined essentially by demanding that the correct mass of ^{56}Ni be ejected from the progenitor. Clearly, the estimate of the position of the cut-off was incorrect. Although it is possible that this may be due to an incorrect calculation of the progenitor’s structure, it is more tempting to attribute the problem to some asymmetry in the explosion. If the explosion was asymmetric, similar to what has been suggested for the hypernova SN 1998bw in order to explain its connection with a GRB, it is quite possible that most ^{56}Ni was produced near the beam axis, while away from that axis burning would be less efficient, and would terminate at intermediate elements such as Si or S (Maeda et al. 2000). Clearly one then has to place the mass cut deeper in order to achieve the

require ejected mass of ^{56}Ni . This is also supported by our derived abundance distribution, which suggests that the S abundance is still increasing at the lowest velocities sampled, about 2000km s^{-1} . The abundance distribution as derived from our models is displayed in Figure 9, but we must keep in mind that, since we used homogenised compositions above the photosphere, all sharp composition boundaries are smoothed out. On the other hand, no clear spectral evidence - such as sudden changes in the properties of the lines - is visible for strict abundance stratification.

The presence of an inner density core was also suggested in Paper I to explain the observed deviation of the synthetic light curve computed with model CO100 from the observations at advanced phases: the synthetic light curve has a steeper slope than the observed one, indicating that γ -ray trapping is more efficient than in the model. This could be achieved if ^{56}Ni was distributed deeper than it is in CO100.

10. A NEW LIGHT CURVE MODEL

In order to verify our findings, we used our derived density and abundance distribution and computed a synthetic light curve in spherical symmetry. We used two different codes, one based on Monte Carlo methods and the other, a radiation hydrodynamics code, which was used in the light-curve computation in Paper I.

The Monte Carlo code is based on the simple code developed for SNe Ia described in Cappellaro et al. (1997). γ -ray deposition in the expanding ejecta is computed following the random walk of gamma-ray photons adopting a constant γ -ray opacity $\kappa_\gamma = 0.027\text{cm}^2\text{g}^{-1}$. Once they deposit their energy, the γ -rays are assumed to generate optical photons on the spot. The random walk of the optical photons through the ejecta is then also followed in Monte Carlo, assuming a constant optical opacity κ_{opt} . The Monte Carlo scheme is able to model efficiently the random walk of photons through the ejecta - and thus to take into account the delay between the emission of a photon and its escaping from the SN nebula, which determines the initial shape of the light curve. The value of κ_{opt} depends on the temperature and composition, and it is possible that it changes with time. Thus we had to find a convenient approximate value for this particular model of SN 1997ef. Since κ_{opt} affects the light curve essentially near maximum, we found that a value $\kappa_{opt} = 0.08\text{ cm}^2\text{g}^{-1}$ gives a good fit to the light curve around maximum. This value is smaller than for SNe Ia, as might be expected since line opacity is much stronger in the Fe-dominated ejecta of a SN Ia.

The synthetic light curve in Monte Carlo is compared to the one obtained with the radiation hydrodynamics code. As described in Paper I, the code solves a multi-frequency radiative transfer equation in the fluid's comoving frame, using the Feautrier method iteratively with an approximate Lambda operator. The energy equation of gas plus radiation and the radiation momentum equation are coupled to the transfer equation in order to follow the evolution of gas temperatures. The code also uses average opacities, and the values used were the same as in the Monte Carlo code.

The synthetic bolometric light curves are shown in Figure 10. Except for a slight difference around the maximum,

which is probably to be ascribed to Monte Carlo noise, the codes produce very similar light curves. Therefore, it is safe to use the simple Monte Carlo code in calculating bolometric luminosities if a reasonable opacity is chosen.

The synthetic light curves reproduce our derived bolometric curve reasonably well around maximum. The V light curve can consequently be reproduced if the bolometric correction as resulting from our synthetic spectra is taken into account. In both codes a ^{56}Ni mass of $0.13M_\odot$ was used. In order to achieve a rapid rise of the light curve, consistent with our dating, we had to distribute ^{56}Ni homogeneously throughout the ejecta. Both light curves reproduce the maximum quite well, but their decline on the tail is much too steep. The observed V light curve after about day 60 appears to follow the ^{56}Co decline rate, implying constant and complete deposition of about $0.07M_\odot$ of ^{56}Ni . However, our codes predict for those advanced epochs a deposition fraction of less than 0.5 and steadily decreasing with time.

In Figure 11 we compare the observed velocity of the Si II doublet with the run of v_{ph} as derived from the two light curve codes and with the values used as input for the calculation of the synthetic spectra. The two codes are in good agreement with one another, although the MC values are consistently larger than those of the radiation hydro model. This is probably due to different zoning in the two codes. However, the observed points are lower than both models, and the difference increases with the epoch. The velocities used for the spectral calculations, on the other hand, start lower than the observed values but slowly approach them. This is understandable, as it can be expected that at early times the Si II line forms above the photosphere since it is very strong. Later, as the line becomes weaker, it forms closer and closer to the photosphere. The fact that the value of v_{ph} tends to flatten out at advanced epochs, and does not reproduce the observations, is not new (see, e.g., Iwamoto et al. 1998 on SN 1998bw), and it probably indicates that the assumption of a gray photosphere is not good at advanced epochs. However, the difference at early phases cannot be due to that effect. One possibility is that we have somewhat overestimated the density at the highest velocities in our spectral calculations, where we were guided more by the Ca II IR triplet than by the Si II doublet. Note that the velocity derived from model CO100 in Paper I was much smaller than the observed values. Another possibility is that our assumption of a gray opacity again fails in those outermost layers, as shown perhaps by the fact that only the Ca II IR triplet is active there. Note that all of these remarks apply to a spherically symmetric situation.

Another inconsistency between the light curve and spectral calculations is that if we integrate the Ni mass as the sum of the abundances of Fe, Co and Ni in the various synthetic spectra we obtain an Fe-group mass of only $\sim 0.04M_\odot$ above 2000km s^{-1} , which is much less than what is necessary to power the light curve. It is unlikely that our spectrum synthesis may have given such a large error, especially since the Fe lines are already very strong in most spectra.

So we have a situation where at early times we need more surface ^{56}Ni to power the light curve than we see in the spectra, while at late times the ^{56}Ni we have used to reproduce the light curve at peak does not deposit sufficiently

to reproduce the light curve slope and brightness. The late light curve appears to require the complete deposition of $\sim 0.07M_{\odot}$ of ^{56}Ni . The two problems may be independent, but they may also be related.

One possibility to explain the late light curve behaviour is that, in a spherically symmetric scenario, additional ^{56}Ni ($\sim 0.05M_{\odot}$) could be located deep in the ejecta, below 2000km s^{-1} . If the density is sufficiently high there the γ -rays produced by the decay of this ^{56}Ni may deposit completely. The presence of very low velocity ejecta would further reduce the mass of the expected compact object, and may be in contradiction with the distribution of ^{56}Ni in models of the progenitor evolution and explosion. This would not affect the situation at early times.

Another possibility is that the ejecta may not be spherically symmetric, in either mass or abundance distribution, or both. If some ^{56}Ni is ejected at low velocities together with other elements in some direction, the γ -rays produced by its decay chain could be efficiently trapped even at advanced epochs. The optical photons produced by the thermalization of γ -rays and positrons in this hypothetical high density region would only be able to escape at advanced phases, and so they would have little effect on the early time spectra but they could power the late light curve. At the same time, some material has been ejected at high velocity, possibly in a jet-like form, to reproduce the sharp rise of the light curve by high-velocity ^{56}Ni and to explain the broad lines of Si II and Ca II ($\sim 20,000\text{km s}^{-1}$) at early epochs. In this scenario, the uniform mixing of ^{56}Ni which was used to reproduce the sharp rise of the light curve might refer only to the ^{56}Ni ejected in the jet, while the low velocity ^{56}Ni would enter play only later.

This scenario might help explaining the discrepancy between the light curve and spectroscopic ^{56}Ni masses. If most of the ^{56}Ni is ejected in a preferred direction (e.g. in the jet that might be observed as a GRB if the viewing angle is favourable), this ^{56}Ni may power the early light curve by depositing its γ -rays in the neighbouring ejecta, which have lower velocity, higher density and a smaller Fe-group abundance. However, if we view the event from an angle sufficiently far from the jet direction, the spectrum we see would be produced in a region where the abundances are different from those found in the jet – hence the smaller spectroscopic mass of ^{56}Ni . This is a possibility for SN 1997ef, since there is no positive identification of a GRB counterpart to the SN event.

The possibility that the explosion was asymmetric is in line with existing models of energetic supernova explosions linked to GHRB's (MacFadyen & Woosley 1999, Höflich et al. 1999, Khokhlov et al. 1999, Maeda et al. 2000), and it deserved further study with multi-dimensional radiation hydrodynamics codes.

11. DISCUSSION

We have shown in this paper how spectrum synthesis can be used not only to verify explosion models of SNe, but also to improve on them. Given our findings, it would now be very interesting to see hydrodynamic calculations of the explosion, in one or more dimensions, which reproduce closely the observed bolometric light curve. The derived density distribution, ejecta mass and kinetic energy may or may not be close to what we have obtained spectroscopically, but in any case such a model would have to

be tested also for its ability to reproduce the SN spectral evolution. Our study also shows that fitting an observed V curve with a synthetic bolometric one may be somewhat misleading, since the bolometric correction can be significant.

We have discussed in §9 the reason for the difference between the density distribution derived from spectral modelling and that obtained from 1D hydrodynamic calculations of the explosion of the stripped core of a massive star, and remarked that the presence of significant amounts of ejected matter at low velocity may be due to some asymmetry in the explosion. A similar conclusion was reached for the other Type Ic hypernova, SN 1998bw, but in that case it was based on somewhat different evidence, most importantly the connection with a GRB (e.g. Wheeler 2000).

The early-time spectra of SN 1998bw have even broader and more blended lines than those of SN 1997ef, but a clear evolution towards lower line velocities and less line blending is not seen as clearly as in SN 1997ef, while the relatively early development of nebular emission is seen in both objects. This may be understandable since although the ejecta mass of SN 1998bw was larger than that of SN 1997ef, even if we use our upwards revised value for the latter, the kinetic energy of SN 1998bw appeared to be much larger (Nomoto et al. 2000). Branch (2000) in a spectroscopic study similar to the one he performed for SN 1997ef, suggested an extremely large KE for SN 1998bw ($6 \cdot 10^{52}\text{erg}$ above 7000km s^{-1} , i.e. a factor 2 larger than his value for SN 1997ef above the same velocity). We have performed a preliminary analysis of SN 1998bw using the technique described in this paper, and find a similarly large value (Nakamura et al. 1999).

If SN 1997ef was also a highly asymmetric explosion, although weaker in energy and ejecting a smaller mass than SN 1998bw, why was a GRB not positively detected? The most likely possibilities are that either the jet-axis of SN 1997ef was not oriented exactly along the line-of-sight, or that a weaker explosion energy reduced the beaming so that a GRB was not formed. Both scenarios might be able to explain many of the observed features of SN 1997ef, in particular the lower expansion velocities and the smaller measured KE . When we apply a spherically symmetric model, we estimate KE by integrating a 1D model around a sphere. Therefore, if the SN is observed on or very close to the jet-axis, like SN 1998bw, KE could be grossly overestimated (Höflich et al. 1999). On the other hand, the difference between the velocity of the spectral lines in the two SNe is real, and so is the difference in luminosity at late times. That SN 1998bw produced more ^{56}Ni is also confirmed by the estimate for the ^{56}Ni mass ($\sim 0.6M_{\odot}$) obtained from the nebular lines, which does not depend much on the asymmetry (see Danziger et al. 1999; Nomoto et al. 2000). Therefore, even though inclination may be a factor, that there is some intrinsic difference between the two objects appears unavoidable, at least as long as the relative distance estimate is reliable.

Finally, we note that another SN 1997ef-like Type Ic hypernova was recently observed, SN 1998ey, whose spectra appear to be identical to those of SN 1997ef, and for which there is also no observed GRB counterpart (Garnavich et al. 1998). This coincidence is striking, and calls for the accumulation of more data on Type Ic hypernova candidates.

Acknowledgements This work has been supported in part by the grant-in-Aid for Scientific Research (12640233, 12740122) and COE research (07CE2002) of the Ministry of Education, Science, Culture and Sports in Japan. It is

a pleasure to thank P.Garnavich and J.Danziger for useful communications and the referee, D.Branch, for constructive remarks.

REFERENCES

- Branch D. 2000, in ‘Supernovae and Gamma-Ray Bursts’, ed. M.Livio et al. , Cambridge University Press, Cambridge, in press
 Cappellaro E., Mazzali P.A., Benetti S., et al. 1997, A&A 328, 203
 Danziger I.J., et al. 1999, in The Largest Explosions Since the Big Bang: Supernovae and Gamma Ray Burst, eds. M. Livio, et al. (Baltimore: STScI), 9
 Filippenko, A.V. 1997, ARA&A, 35, 309
 Galama T.J., Vreeswijk P.M., van Paradijs J., et al. 1998, Nat 395 670
 Garnavich P., Jha S., Kirshner R., Challis P. 1997a, IAU Circ. No.6778
 Garnavich P., Jha S., Kirshner R., Challis P., Balam D. 1997b, IAU Circ. No.6786
 Garnavich P., Jha S., Kirshner R., Challis, P. 1997c, IAU Circ. No.6798
 Garnavich P., Jha S., Kirshner R. 1998, IAU Circ. No. 7066
 Germany L.M., Reiss D.J., Schmidt B.P., Stubbs C.W., Sadler E.M. 2000, ApJ, 533, 320
 Höflich P., Wheeler J.C., Wang L. 1999, ApJ 521, 179
 Iwamoto K., Mazzali P.A., Nomoto, K., et al. 1998, Nat 395 672
 Iwamoto K., Nakamura T., Nomoto K., Mazzali P.A., Danziger I.J., Garnavich P., Kirshner R., Jha S., Balam D., Thorstensen, J., 2000, ApJ 534, 660
 Iwamoto, K., Nomoto, K., Höflich, P., Yamaoka, H., Kumagai, S., & Shigeyama, T. 1994, ApJ, 437, L115
 Khokhlov A.M., Höflich P.A., Oran E.S., Wheeler J.C., Wang L., Chtchelkanova A.Yu. 1999, ApJ 524, L107
 Lucy L.B. 1999, A&A 345, 211
 MacFadyen A.I., Woosley S.E., 1999, ApJ 524, 262
 Maeda K., Nakamura T., Nomoto K., Mazzali P.A., Hachisu, I. 2000, in Origin of Matter and Evolution of Galaxies, ed. T. Kajino et al. (Singapore: World Scientific), in press
 Mazzali P.A., 2000, A&A, in press
 Mazzali P.A., Lucy, L.B., 1993, A&A 279, 447
 Mazzali P.A., Schmidt B., 2000, in preparation
 Millard, J., Branch, D., Baron, E., et al. 1999, ApJ, 527, 746
 Nakamura, T., Mazzali, P.A., Nomoto, K., Iwamoto, K., & Umeda, H. 1999, Astron. Nachrichten, 320, 363
 Nakamura, T., Mazzali P.A., Nomoto, K., & Iwamoto, K., 2000, ApJ, submitted (astro-ph/0007010)
 Nomoto K., Filippenko A.V., Shigeyama T., 1990, A&A 240, L1
 Nomoto, K., Yamaoka, H., Pols, O. R., van den Heuvel, E. P. J., Iwamoto, K., Kumagai, S., & Shigeyama, T. 1994, Nature, 371, 227
 Nomoto, K., Mazzali, P., Nakamura, T., Iwamoto, K., Maeda, K., Suzuki, T., Turatto, M., Danziger, I.J., & Patat, F. 2000, in ‘Supernovae and Gamma-Ray Bursts’, ed. M. Livio et al. , Cambridge University Press, Cambridge, in press (astro-ph/0003077)
 Patat F., Benetti S., Cappellaro E., et al., 1996, MNRAS 278, 111
 Swartz D.A., Filippenko A.V., Nomoto K., Wheeler J.C., 1993, ApJ 411, 313
 Wang L., Wheeler J.C., 1998, ApJ 504, L87
 Wheeler J.C., 2000, in ‘Supernovae and Gamma-Ray Bursts’, ed. M. Livio et al. , Cambridge University Press, Cambridge, in press
 Woosley, S. E., Eastman, R. G., & Schmidt, B.P. 1999, ApJ, 516, 788

TABLE 1
PARAMETERS OF THE SYNTHETIC SPECTRA

date	epoch days	L erg s ⁻¹	v_{ph} km s ⁻¹	$v(\text{Si II})$ R_{\odot}	$\log \rho_{ph}$ g cm ⁻³	Mass M_{\odot}	T_{eff} K	T_{bb} K	B_{mod}	V_{mod}	V_{obs}	BC	M_{mod}
29 Nov	9	42.13	15500	19072	-12.65	1.05	6123	7725	17.45	16.74	16.7	0.29	-16.600
5 Dec	15	42.15	9500	13962	-12.30	3.38	6128	9447	17.35	16.58	16.5	0.40	-16.650
17 Dec	27	42.20	7500	8011	-12.67	5.16	5291	6648	17.72	16.65	16.6	0.20	-16.775
24 Dec	34	42.13	4900	5378	-12.71	7.56	5602	7602	17.83	16.71	16.8	0.32	-16.500
1 Jan	42	42.00	3600	3775	-12.78	8.48	5426	6830	18.41	17.16	17.3	0.22	-16.250
26 Jan	67	41.80	1950	-	-13.51	8.97	5232	5701	19.06	17.85	18.0	0.01	-15.775

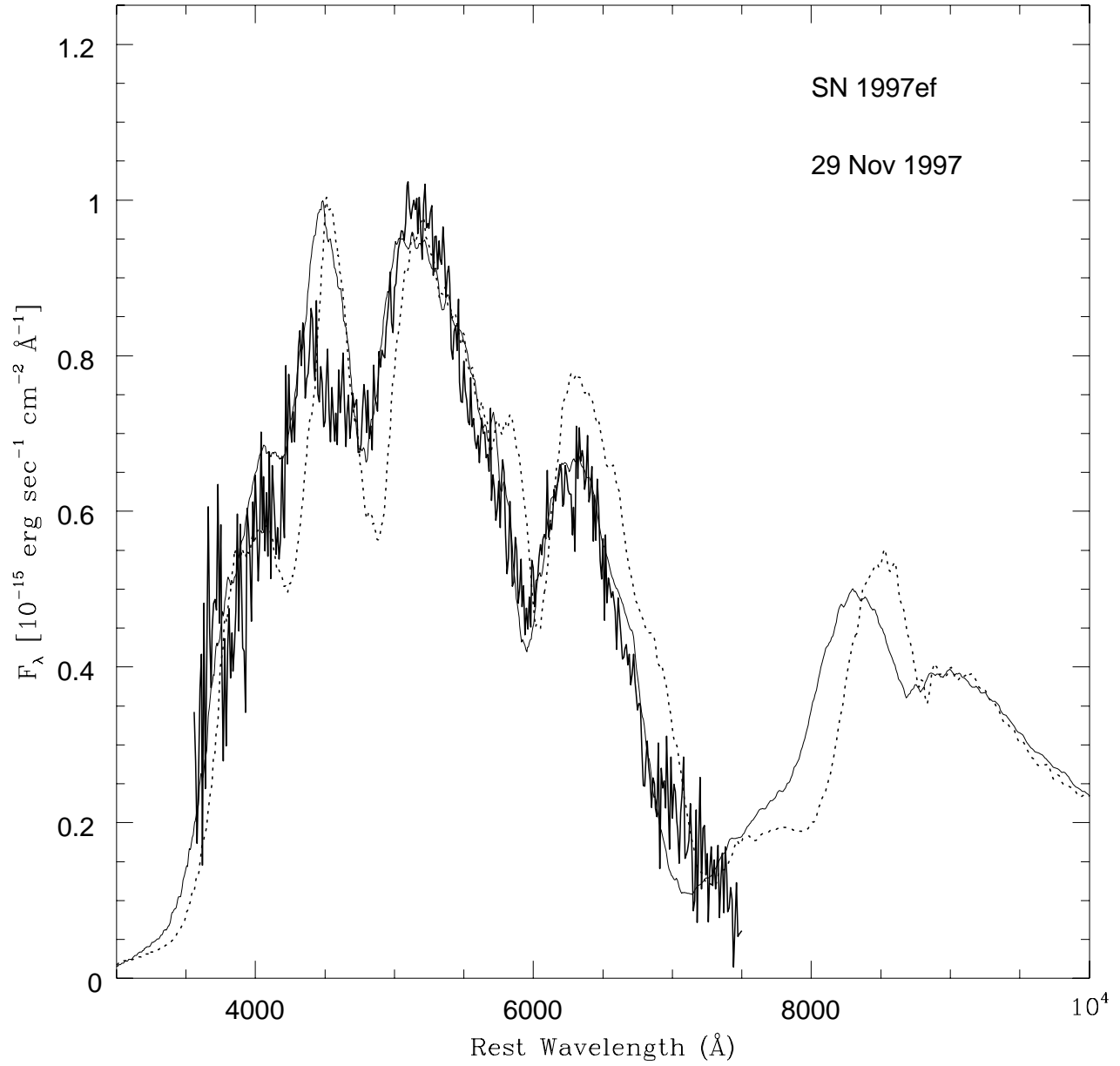


FIG. 1.— The observed, smoothed spectrum of SN 1997ef on Nov 29, 1997 (thick line), compared to two synthetic spectra computed with the CO100 ad hoc density structure. The fully drawn thin line is a spectrum computed for $t = 9$ days, while the dashed line is a spectrum computed for $t = 11$ days.

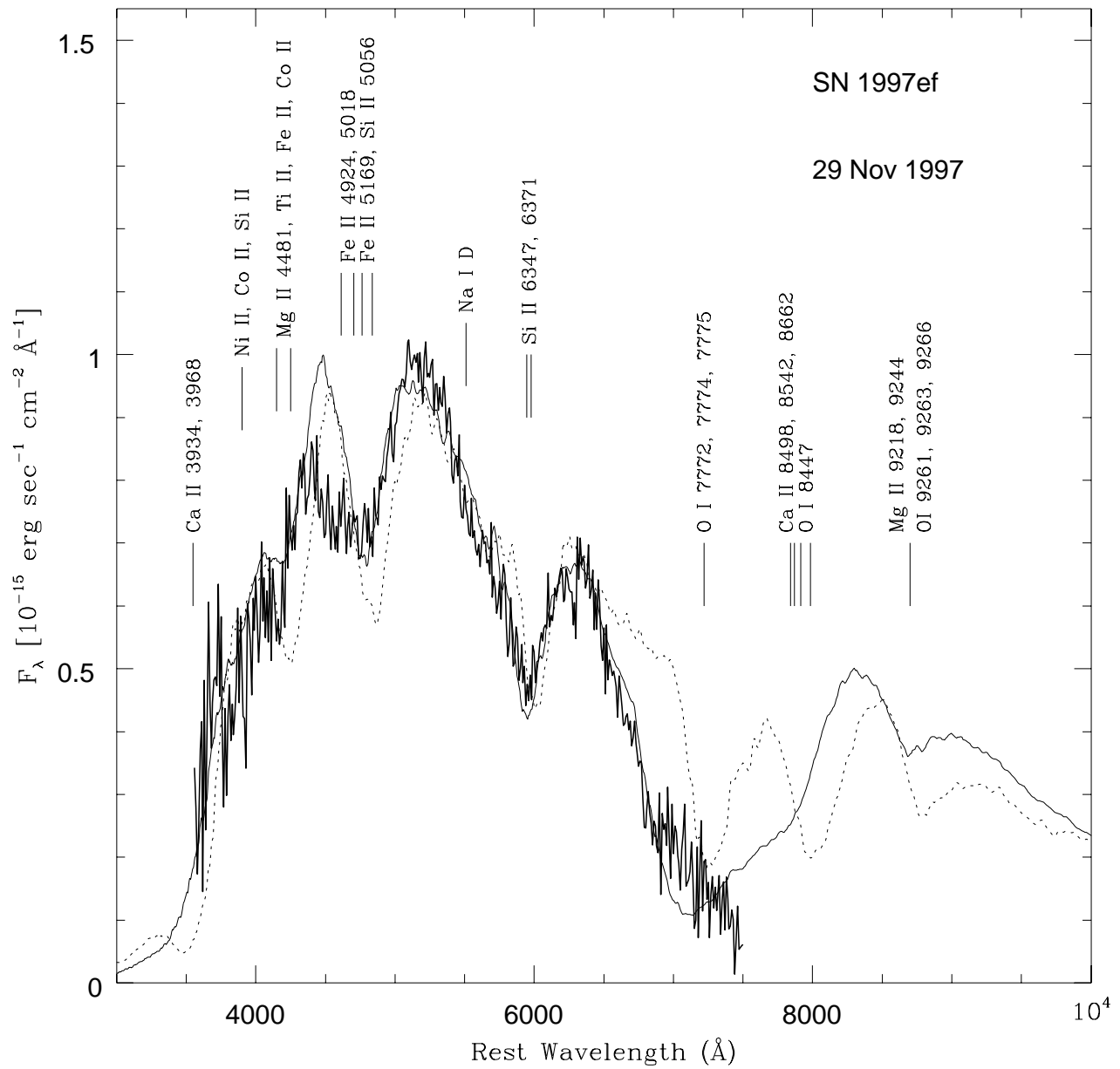


FIG. 2.— The observed, smoothed spectrum of SN 1997ef on Nov 29, 1997 (thick line), compared to two synthetic spectra computed for $t = 9$ days. The dashed line is a spectrum computed with the original model CO100, while the fully drawn thin line is a spectrum computed with the modified outer density described in the text.

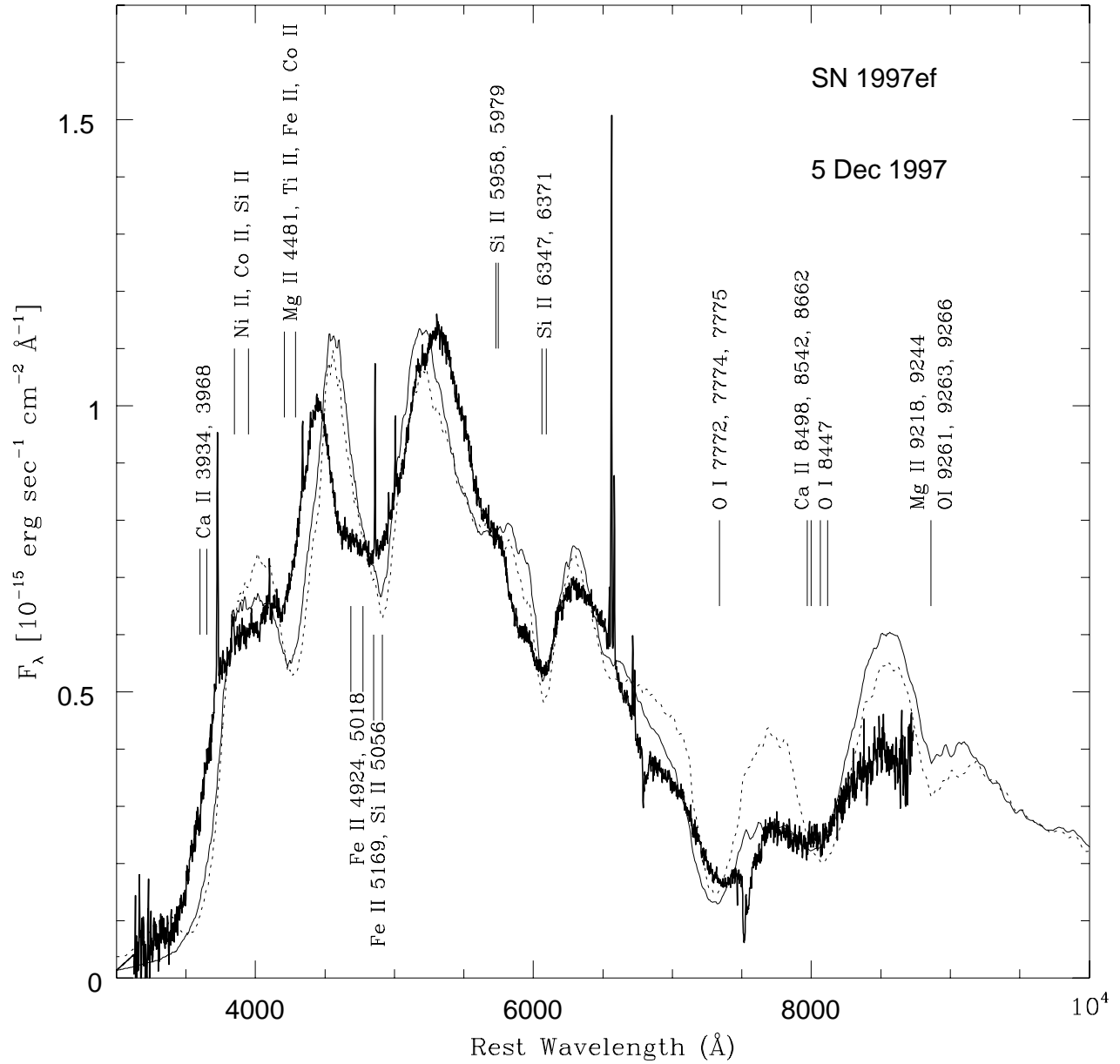


FIG. 3.— The observed spectrum of SN 1997ef on Dec 5, 1997 (thick line), compared to two synthetic spectra computed for $t = 15$ days. The dashed line is a spectrum computed with the original model CO100, while the fully drawn thin line is a spectrum computed with the modified outer density described in the text.

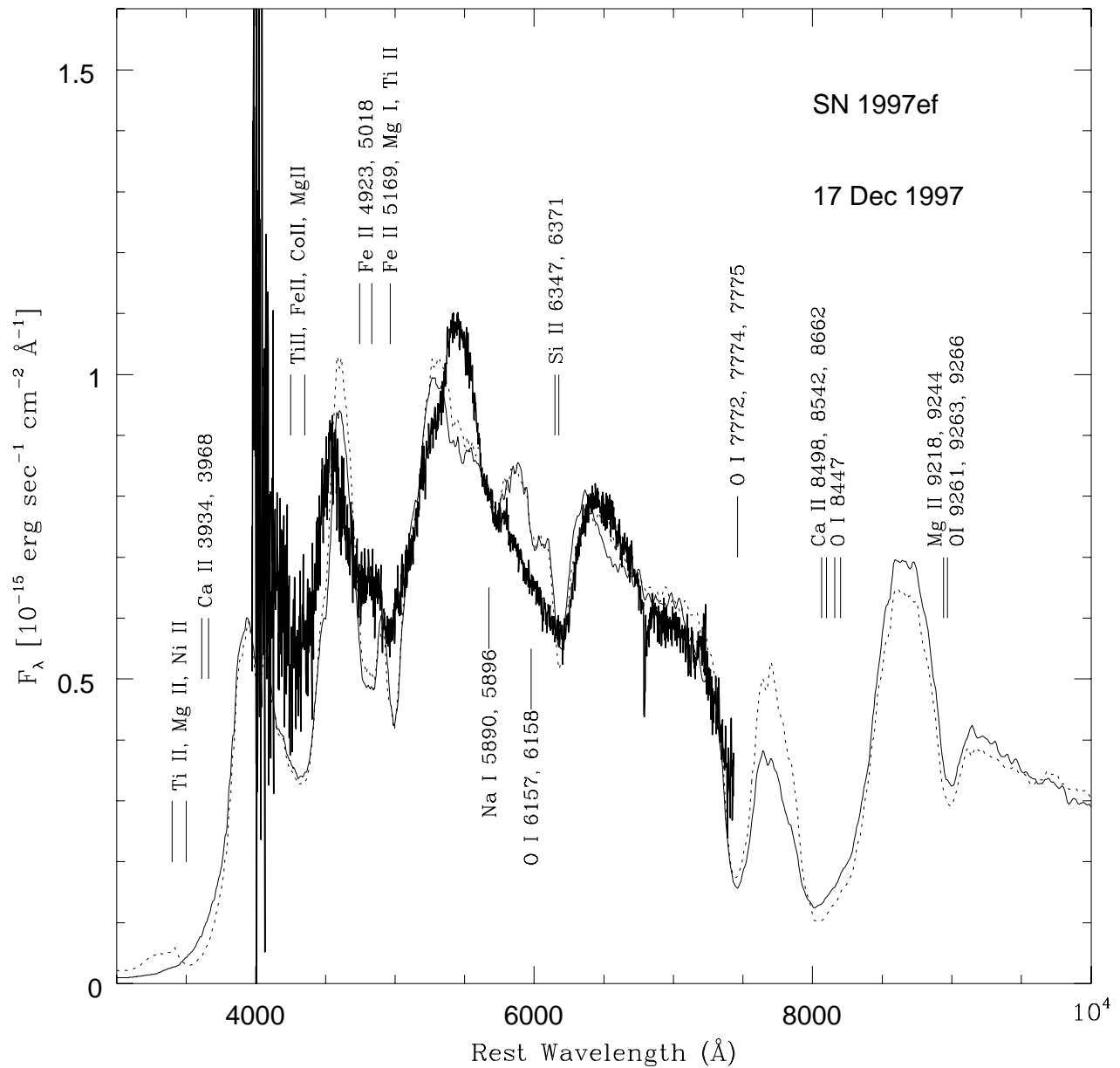


FIG. 4.— The observed spectrum of SN 1997ef on Dec 17, 1997 (thick line), compared to two synthetic spectra computed for $t = 27$ days. The dashed line is a spectrum computed with the original model CO100, while the fully drawn thin line is a spectrum computed with the modified outer density described in the text.

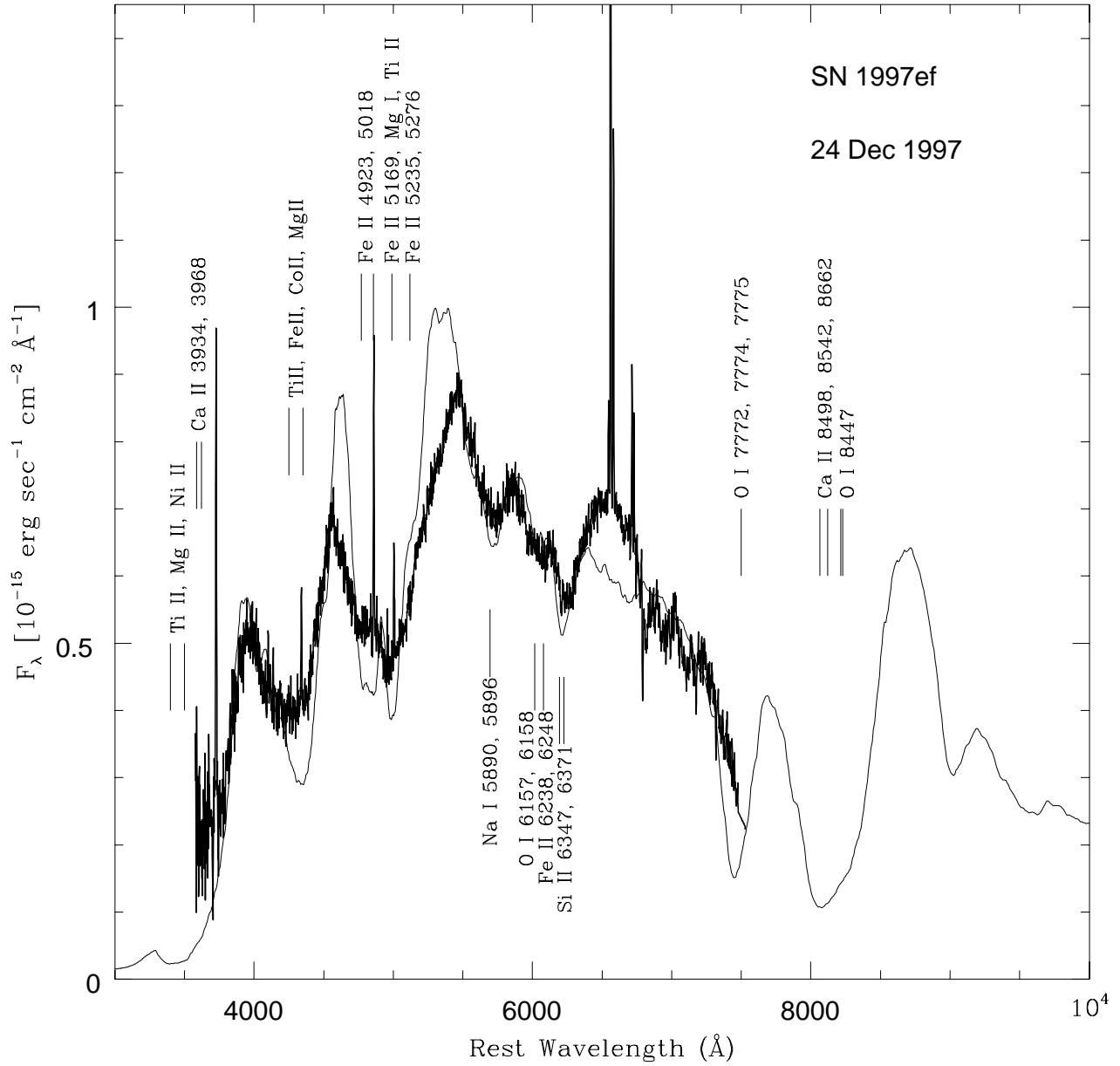


FIG. 5.— The observed spectrum of SN 1997ef on Dec 24, 1997 (thick line), compared to a synthetic spectra computed for $t = 34$ days using the modified density described in the text (thin line).

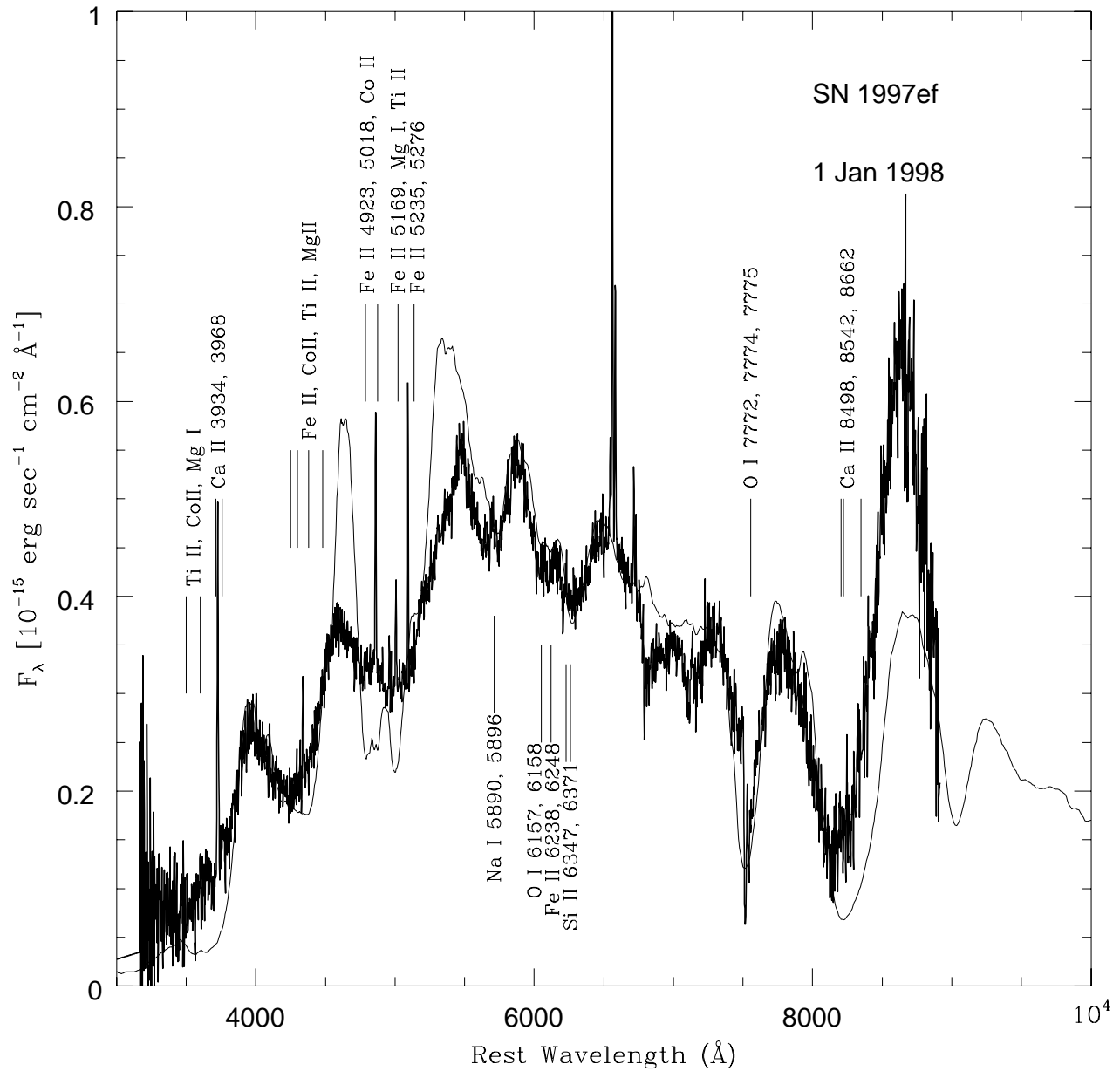


FIG. 6.— The observed spectrum of SN 1997ef on Jan 1, 1998 (thick line), compared to a synthetic spectra computed for $t = 42$ days using the modified density described in the text (thin line).

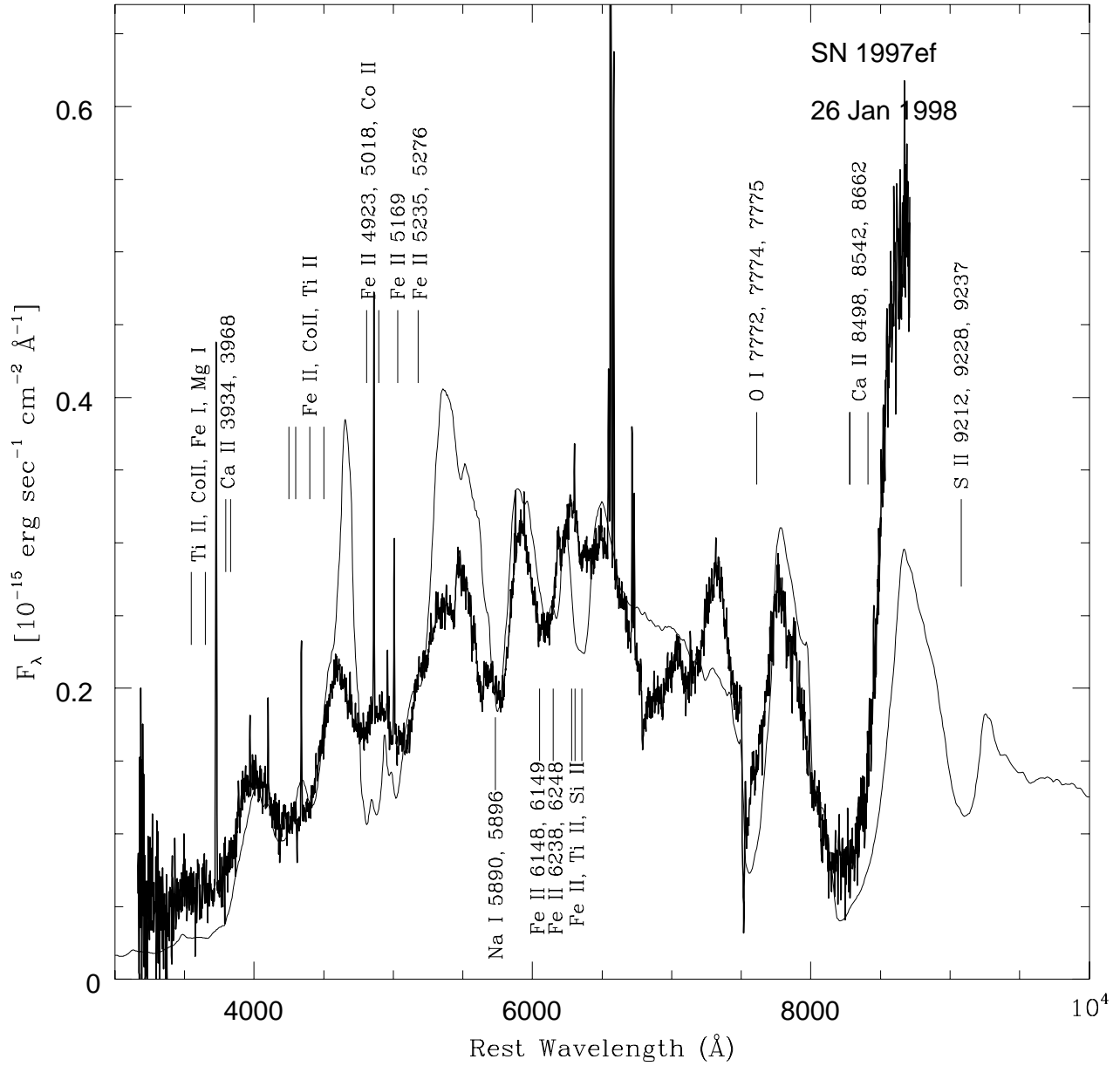


FIG. 7.— The observed spectrum of SN 1997ef on Jan 26, 1998 (thick line), compared to a synthetic spectra computed for $t = 67$ days using the modified density described in the text (thin line).

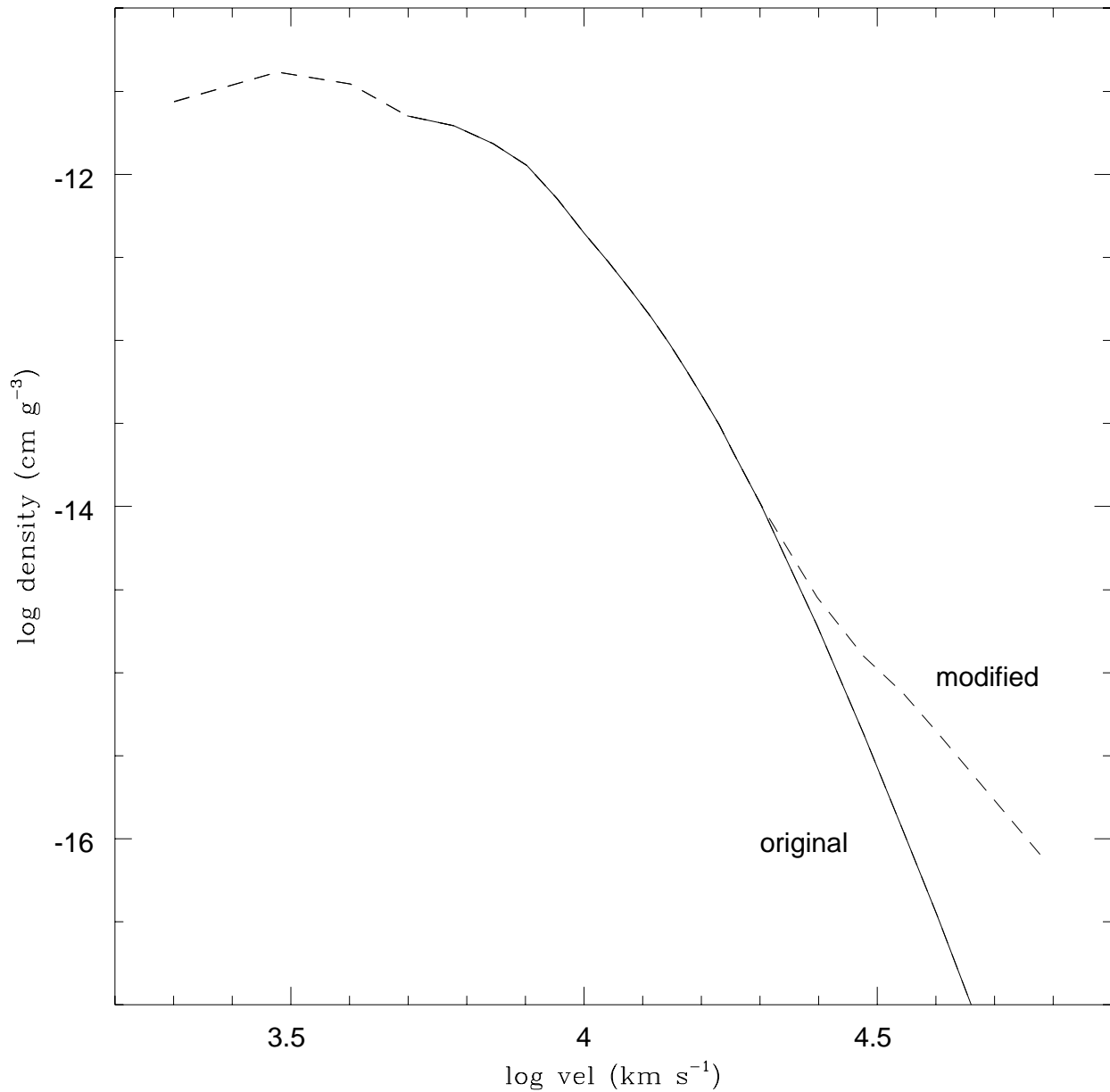


FIG. 8.— The original density structure of the hydrodynamical model CO100 (continuous line) and the modifications introduced to improve the spectral fits (dashed line). The outer part of the modified density structure has a power law index $n = -4$, while the inner extension has $n = 1$ between $v = 3000$ and $v = 5000$ km s^{-1} and $n = -1$ below $v = 3000$ km s^{-1} .

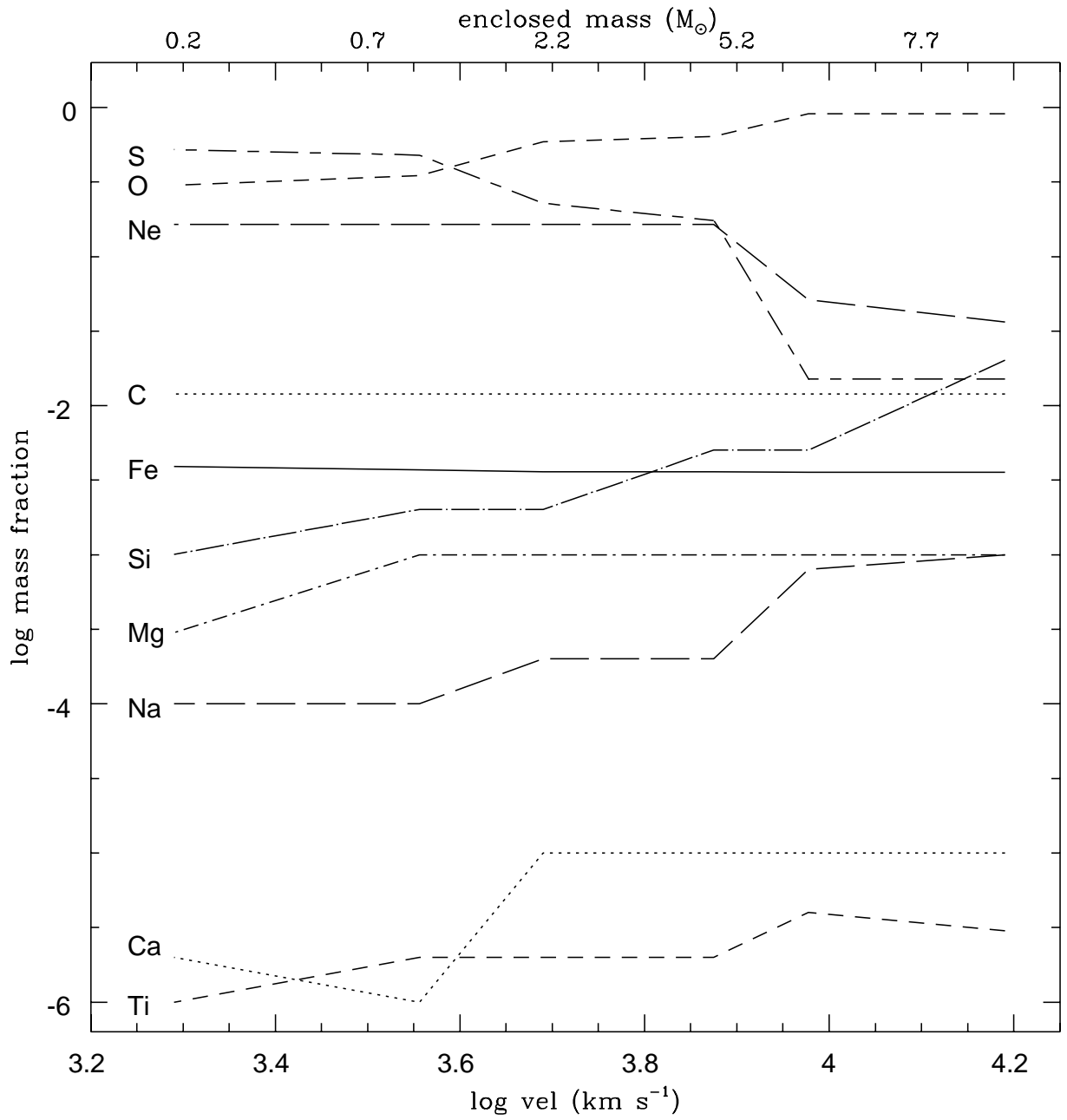


FIG. 9.— Composition structure in the ejecta of SN 1997ef as derived from spectrum synthesis.

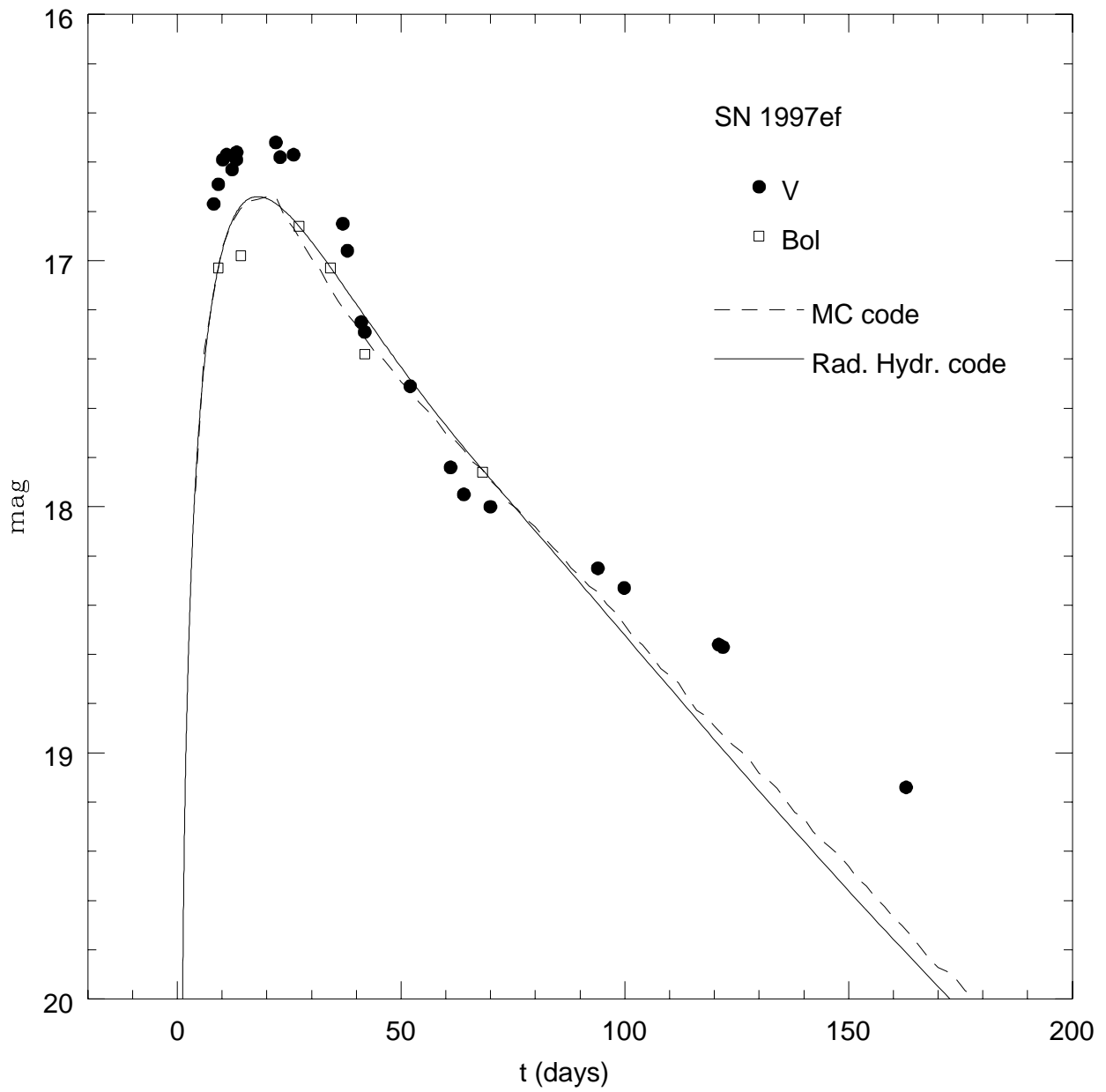


FIG. 10.— The synthetic bolometric light curves computed with the Monte Carlo and the radiation hydrodynamics codes using the density distribution derived from our spectral fits, compared to the quasi-bolometric light curve of SN 1997ef.

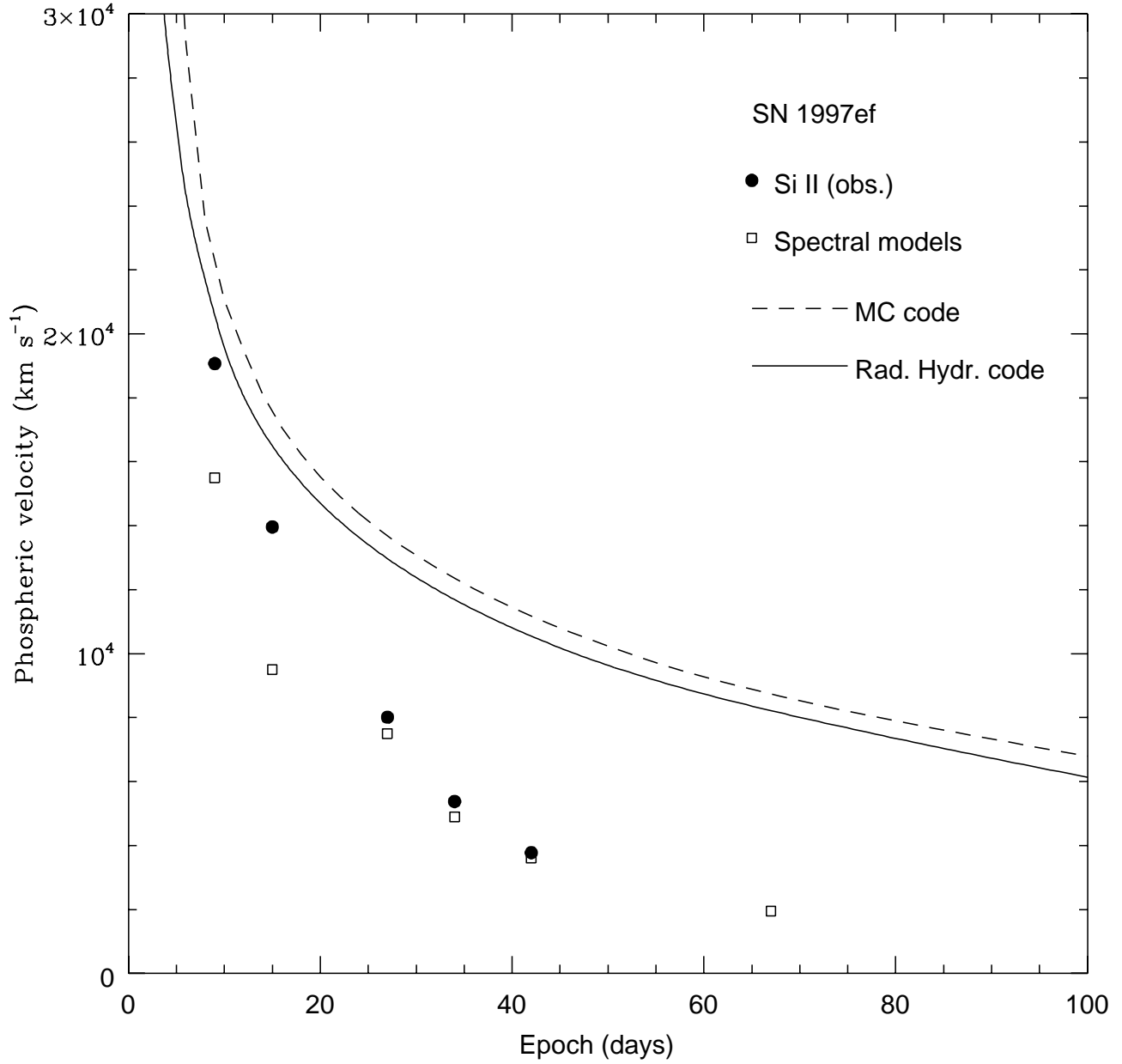


FIG. 11.— The evolution of the velocity of the observed Si II doublet and of the photospheric velocity as computed by the two light curve codes and as derived from the spectral calculations.